Molecular Pharmacology Fast Forward. Published on June 26, 2009 as doi:10.1124/mol.109.055830
This article has not been copyedited and formatted. The final version may differ from this version.

MOL 55830

Dual Mechanisms of sHA 14-1 in Inducing Cell Death through Endoplasmic Reticulum and Mitochondria*

David Hermanson, Sadiya N. Addo, Anna A. Bajer, Jonathan S. Marchant, Sonia Goutam Kumar Das, Balasubramanian Srinivasan, Fawaz Al-Mousa, Francesco Michelangeli, David D. Thomas, Tucker W. LeBien, Chengguo Xing

Department of Medicinal Chemistry (D.H., S.N.A., S.G.D., B.S., C.X.); Department of Laboratory Medicine and Pathology (A.A.B., T.W.L.); Department of Pharmacology (J.S.M.); Department of Biochemistry, Molecular Biology and Biophysics (D.D.T.), Masonic Cancer Center- University of Minnesota (T.W.L., C.X.), Minneapolis, MN 55455; and School of Biosciences, University of Birmingham, Edgbaston, Birmingham UK B15 2TT (F.A., F.M.)

Molecular Pharmacology Fast Forward. Published on June 26, 2009 as DOI: 10.1124/mol.109.055830
This article has not been copyedited and formatted. The final version may differ from this version.

Running title: sHA 14-1 inhibits SERCAs and antagonizes Bcl-2 family proteins

Corresponding author:

Chengguo Xing, Ph.D.

308 Harvard St SE

Minneapolis, MN 55455

Phone: 612-626-5675

Fax: 612-624-0139

E-mail: xingx009@umn.edu

Number of text pages:

Number of tables: 0

Number of figures: 8

Number of References: 67

Number of words in Abstract: 243

Number of words in Introduction: 544

Number of words in Discussion: 1266

A list of nonstandard abbreviation used in the paper

ER, endoplasmic reticulum; IP_3R, inositol triphosphate receptor; SERCA, sarco-endoplasmic reticulum Ca(2+)-ATPase; FCCP, carbonylcyanide-4-(trifluromethoxy)-phenylhydrazone; ATF4, activating transcription factor 4; ALL, acute lymphoblastic leukemia; CLM, cytosol like medium; SR, sarcoplasmic reticulum; PI, propidium iodide; $\Delta\psi m$, mitochondrial transmembrane potential; TMRE, tetramethylrhodamine; ROS, reactive oxygen species.

Molecular Pharmacology Fast Forward. Published on June 26, 2009 as DOI: 10.1124/mol.109.055830
This article has not been copyedited and formatted. The final version may differ from this version.

Abstract

HA 14-1 is a small-molecule Bcl-2 antagonist that promotes apoptosis in malignant cells, but its mechanism of action is not well defined. We recently reported that HA 14-1 has a half-life of only 15 min in vitro, which led us to develop a stable analog of HA 14-1 (sHA 14-1). The current study characterizes its mode of action. Because of the anti-apoptotic function of Bcl-2 family proteins on the endoplasmic reticulum (ER) and mitochondria, the effect of sHA 14-1 on both organelles was evaluated. sHA 14-1 induced ER calcium release in human leukemic cells within 1 min, followed by induction of the ER stress inducible transcription factor, ATF4. Similar kinetics and stronger intensity of ER calcium release were induced by the sarco-endoplasmic reticulum Ca(2+)-ATPase (SERCA) inhibitor, thapsigargin, accompanied by similar kinetics and intensity of ATF4 induction. sHA 14-1 directly inhibited SERCA enzymatic activity but had no effect on the inositol triphosphate receptor (IP_3R). Evaluation of the mitochondrial pathway showed that sHA 14-1 triggered a loss of mitochondrial transmembrane potential ($\Delta\psi m$) and weak caspase-9 activation, whereas thapsigargin had no effect. ABT-737, a well-established small-molecule Bcl-2 antagonist, rapidly induced loss of $\Delta\psi m$ and caspase-9 activation, but had no effect on the ER. The pan-caspase inhibitor Z-VAD-fmk had some protective effect on sHA 14-1 induced cell death. These collective results suggest a unique dual targeting mechanism of sHA 14-1 on the apoptotic resistance machinery of tumor cells that includes anti-apoptotic Bcl-2 family proteins and SERCA proteins.

Molecular Pharmacology Fast Forward. Published on June 26, 2009 as DOI: 10.1124/mol.109.055830
This article has not been copyedited and formatted. The final version may differ from this version.

Drug resistance is a major challenge in the treatment of cancer. At the molecular level, one major mode to acquire drug resistance is through the over-expression of anti-apoptotic Bcl-2 family proteins (Adams and Cory, 2007; Reed, 2003), which leads to the suppression of apoptosis. Since inducing apoptosis is a key mechanism by which most anticancer drugs eliminate tumor cells, antagonizing anti-apoptotic Bcl-2 family proteins is a promising approach in overcoming drug resistance.

Anti-apoptotic Bcl-2 family proteins can localize to various organelles, including mitochondria, endoplasmic reticulum (ER), and nucleus (Rong and Distelhorst, 2008; Krajewski *et al.*, 1993). Although the function of nuclear Bcl-2 proteins is uncertain, the functions and mechanisms of these proteins localized to mitochondria and ER in apoptotic regulation are better understood. The mitochondria-localized anti-apoptotic Bcl-2 family proteins antagonize pro-apoptotic stimuli, prevent mitochondrial depolarization, and suppress the release of pro-apoptotic molecules critical for apoptosis, such as cytochrome *c* (Ow *et al.*, 2008). The ER-localized anti-apoptotic Bcl-2 family proteins suppress apoptosis through regulating calcium homeostasis and preventing sustained cytosolic calcium increases, although the exact mechanism is unsettled (Rong and Distelhorst, 2008; Breckenridge *et al.*, 2003; Giorgi *et al.*, 2008; Xu *et al.*, 2005). Recent studies suggest that ER-localized anti-apoptotic Bcl-2 family proteins may regulate calcium homeostasis through modulating ER-localized calcium transporters, including inositol phosphate 3 receptor (IP_3R)(Chen *et al.*, 2004; Li *et al.*, 2002; White *et al.*, 2005; Hanson *et al.*, 2008; Li *et al.*, 2007) and sarco-endoplasmic reticulum Ca(2+)-ATPase (SERCA) (Kuo *et al.*, 1998; Dremina *et al.*, 2006; Dremina *et al.*, 2004), both of which have been reported to be responsible for drug resistance against certain types of cancer therapies (Lee *et al.*, 2007; O'Neill *et al.*, 2006; Denmeade and Isaacs, 2005; Bollig *et al.*, 2007; Liu *et al.*, 2008).

During the past few years, dozens of small-molecule Bcl-2 protein antagonists have been discovered, and several have entered clinical trials for treatment of hematopoietic malignancies and solid tumors (Doshi and Xing, 2008; Letai, 2005; Reed, 2008). HA 14-1 (Fig. 1) was the first small-molecule Bcl-2 antagonist reported (Wang *et al.*, 2000), and this compound demonstrated selective cytotoxicity against drug-resistant cancer cells that over-express anti-apoptotic Bcl-2 family proteins (Dai *et al.*, 2004; Lickliter *et al.*, 2003). Furthermore, numerous studies have reported synergism of HA 14-1 with cancer therapies of diverse mechanisms of action (Pei *et al.*, 2003; Sinicrope *et al.*, 2004; Nimmanapalli *et al.*, 2003; Pei *et al.*, 2004; Sinicrope and Penington, 2005; Milella *et al.*, 2004; Manero *et al.*, 2006; Niizuma *et al.*, 2006; Milella *et al.*, 2002; An *et al.*, 2007; Lickliter *et al.*, 2007), suggesting the potential utility of HA 14-1 in combination therapy for cancer treatment. However, HA 14-1 is highly unstable and rapidly decomposes to inactive species with a half-life of only 15 min in cell culture medium (Doshi *et al.*, 2007). Because of this highly undesirable instability, we synthesized a stable analog of HA 14-1, designated sHA 14-1, which also exhibits synergism and selective toxicity against Bcl-2 over-expressing drug-resistant

Molecular Pharmacology Fast Forward. Published on June 26, 2009 as DOI: 10.1124/mol.109.055830
This article has not been copyedited and formatted. The final version may differ from this version.

cancer cells (Tian *et al.*, 2008). The goal of the present study was to elucidate the molecular mechanism of sHA 14-1 in inducing apoptosis. We show that sHA 14-1 has a dual mode of action that involves antagonizing mitochondrial Bcl-2 proteins and inhibits SERCA proteins and induces ER stress.

Materials and Methods

Chemicals and Reagents. The stable analog of HA 14-1, sHA 14-1 [Ethyl-2-amino-6-phenyl-4-(2-ethoxy-2-oxoethyl)-4*H*-chromene-3-carboxylate] (Fig. 1), was synthesized and characterized by NMR and mass spectrometry, as previously described (Tian *et al*., 2008). An inactive variant of sHA 14-1, designated isHA 14-1, was synthesized and characterized following a similar procedure (Fig. 1). isHA 14-1 differs from sHA 14-1 with the 4'-ethyl replaced by a morpholinyl group (Fig. 1). ABT-737 (Fig. 1) was synthesized following published procedures (Oltersdorf *et al.*, 2005). Fura-2AM was from Invitrogen (Carlsbad, CA). Thapsigargin (Fig. 1) was obtained from Acros Organics (Geel, Belgium). EGTA-AM was from VWR Scientific (Batavia, IL). Carbonylcyanide-4-(trifluoromethoxy)-phenylhydrazone (FCCP), and probenecid were from Sigma-Aldrich (St Louis, MO). $^{45}Ca^{2+}$ (27 mCi/ml) was from PerkinElmer (Boston, MA). CellTiter Blue Assay Kit was from Promega (Madison, WI). The anti-activating transcription factor-4 (ATF-4) antibody (cat #200) was from Santa Cruz Biotechnology, Inc. (Santa Cruz, CA) and was used at a final dilution of 1:500. The anti-Bcl-2 antibody (cat #B3170) was from Sigma Aldrich and was used at a final dilution of 1:1000. The anti-caspase-9 antibody was from Cell Signaling (Boston, MA, cat #9761) and was used at a final dilution of 1:1000.

Cell Culture and Treatment. JURKAT and U937 human leukemic cell lines were obtained from the ATCC. The human B-lineage acute lymphoblastic leukemia (ALL) cell lines BLIN-1 (Wörmann *et al.*, 1989), RS4;11 (Stong *et al.*, 1985), and NALM-6 (Hurwitz *et al.*, 1979) were either originally established or originally characterized at the University of Minnesota. All human leukemic cell lines were maintained in RPMI-1640 (+) L-Glutamine supplemented with 10% fetal bovine serum and 1% penicillin/streptomycin. The chicken DT-40 B lymphoma cell line and IP_3R *null* DT-40 cell line (Sugawara *et al.*, 1997) were kindly provided by Dr. Chi Li (University of Louisville, Louisville, KY). Both DT-40 cell lines were cultured in RPMI-1640 (+) L-Glutamine supplemented with 10% FBS and 1% chicken serum, and 1% penicillin/streptomycin. All cell lines were incubated at 37 °C with 5 % CO_2 in air atmosphere.

Evaluation of Cell Viability. Leukemic cells were plated at a density of 1 x 10^4 cells/well in a 96-well round-bottom plate. Test compounds were added at varying concentrations in 1% DMSO and cells treated with medium containing 1% DMSO served as a control. After a 24-h treatment, relative cell viability in each well was determined using the CellTiter-Blue Cell Viability Assay. The IC_{50} of each compound was

Molecular Pharmacology Fast Forward. Published on June 26, 2009 as DOI: 10.1124/mol.109.055830
This article has not been copyedited and formatted. The final version may differ from this version.

determined by fitting the relative viability of the cells to the drug concentration, using a dose-response model in Prism program from GraphPad Software, Inc. (San Diego, CA).

Determination of Cytosolic Calcium Concentration. Cells at a density of 1 x 10^6 cells/mL were incubated in medium containing 5 μM Fura-2AM and 2.5 mM probenecid at room temperature in the dark for 30 min. The cells were then washed once with cold PBS and re-suspended to a concentration of 2 x 10^6 cells/mL in medium containing 2.5 mM probenecid. To a cuvette with 735 μL media containing 100 mM EGTA and 2.5 mM probenecid was added 750 μL of the cell suspension. The cell suspension was mixed by a slow stirring magnetic bar. Under this condition, the cell medium contained negligible amount of free calcium. Therefore the cells had no extracellular calcium source. Fluorescence emission was measured for 1 min followed by adding 15 μL medium containing sHA14-1, and readings were continued for another 9 min. Readings were obtained on a dual wavelength fluorometer (Cary Eclipse, Varian, Palo Alto, CA) with excitation wavelengths alternating between 340 and 380 nm and an emission wavelength of 510 nm.

The effect of sHA 14-1 on Thapsigargin-Induced ER Calcium Release. This experiment followed the same procedures as that for *Determination of Cytosolic Calcium Concentration*, except that extracellular calcium was not chelated by EGTA in this assay.

$^{45}Ca^{2+}$ Assays. NALM-6 cells (1 x 10^8cells/ml) were suspended in 25 ml calcium free medium (140 mM KCl, 20 mM NaCl, 2 mM $MgCl_2$, 1 mM EGTA and 20 mM PIPES, pH = 7 at 37°C). The cells were incubated in a gyratory waterbath and permeabilized by adding 5 μL increments of 10 μg/ml saponin, and membrane permeability was monitored by trypan blue staining. Permeabilized cells were centrifuged and re-suspended in 6 ml of cytosol-like medium [CLM: 140 mM KCl, 20 mM NaCl, 2 mM $MgCl_2$, 1 mM EGTA, 300μM $CaCl_2$ (free [Ca^{2+}] ~200nM and 20 mM PIPES, pH = 7 at 37°C]. For loading experiments, cells were separated into two tubes, one of which contained DMSO and the other of which contained sHA 14-1 (50 μM), and then incubated with $^{45}Ca^{2+}$ (~5μCi/ml) in the presence of FCCP (10 μM). A cell sample containing 10 μM thapsigargin was used as the background control. At appropriate times, 200 μl aliquots were transferred to separate tubes with the addition of 5 mM ATP. Incubations were terminated by filtration over GF/C filters, washed with sucrose/citrate solution [310 mM sucrose, 1 mM trisodium citrate]. The filter discs were collected, soaked in scintillation liquid overnight, and the radioactive counts quantified the following day. Ca^{2+}uptake was then plotted in the absence and presence of sHA 14-1 using GraphPad Prism 4, using thapsigargin treated sample as the background radioactive counts. For Ca^{2+} release assays, NALM-6 or U937 cells (1 x 10^8 cells/ml) were permeabilized as described above and resuspended in 6 mL of CLM containing 10 μM of FCCP, 5 mM ATP and 6 μL of $^{45}Ca^{2+}$. After loading to steady state (~10 min), samples (200 μL) were transferred into tubes containing different concentrations of

Molecular Pharmacology Fast Forward. Published on June 26, 2009 as DOI: 10.1124/mol.109.055830
This article has not been copyedited and formatted. The final version may differ from this version.

either IP_3 or sHA 14-1. Following a 5-min incubation the cells were filtered over GF/C filter paper and processed as described above.

Measurement of SERCA Enzymatic Activity. Rabbit skeletal muscle sarcoplasmic reticulum (SR) Ca^{2+} ATPase was used as a source of SERCA1A, and enzymatic activity measured using a coupled enzymatic assay as previously described (Michelangeli and Munkonge, 1991). Pig brain microsome Ca^{2+} ATPase (Bilmen and Michelangeli, 2002) was used as a source of SERCA2B, and enzymatic activity measured using a phosphate liberation assay as previously described (Wootton and Michelangeli, 2006). To prepare highly purified SERCA samples, SR vesicles prepared from fast-twitch skeletal muscle of New Zealand White rabbits (Fernandez *et al.*, 1980) was purified on a discontinuous sucrose gradient (Birmachu *et al.*, 1989) to remove junction SR-containing calcium release channels. The resulting SR was further purified on a reactive red column to produce a preparation in which at least 99% of the protein was SERCA (Reddy *et al.*, 2003).

Flow Cytometric Detection of Apoptotic Cells, Mitochondrial Membrane Depolarization, and Cytochrome C Release. Apoptotic cells were detected by staining with Annexin V and propidium iodide (PI). The loss of mitochondrial transmembrane potential ($\Delta\psi m$) was detected by staining cells with the cationic lipophilic fluorescent dye, tetramethylrhodamine (TMRE), using a FACSCalibur (BD Biosciences, San Jose, CA). Detection of cytochrome *c* was accomplished using the Innocyte™ Flow Cytometric Cytochrome c Release Kit (Calbiochem) according to manufacturer's instructions. All methods were conducted as previously described (Shah *et al.*, 2004).

Western Blotting. Western blotting was conducted using standard chemiluminescent techniques, as previously described (Shah *et al*., 2004). Following a 2-4 h incubation in primary antibody at room temperature the blot was washed and secondary staining was accomplished using the corresponding IgG conjugated to horseradish perioxidase. Protein loading was assessed using anti-beta tubulin or anti-AKT.

Statistics. All biological experiments, including *in vitro* cytotoxicity assays and calcium assays, were performed at least three times. Flow cytometry and Western Blot analyses are representative of many experiments. Data are presented as means ± S.D., and comparisons were made using Student's *t* test. A probability of 0.05 or less was considered statistically significant.

Results

Characterization of Apoptotic Induction by sHA 14-1 and isHA 14-1. Prior to conducting studies on the mechanism of action of sHA 14-1, we examined its capacity to induce apoptosis in several widely used B-lineage ALL cell lines. Overnight incubation with sHA 14-1 (6-100 μM) showed that NALM-6, BLIN-1 and RS4;11 had similar sensitivities, with an IC_{50} of ~ 50 μM (Fig. 1B). Importantly, the inactive

Molecular Pharmacology Fast Forward. Published on June 26, 2009 as DOI: 10.1124/mol.109.055830
This article has not been copyedited and formatted. The final version may differ from this version.

variant isHA 14-1 had absolutely no pro-apoptotic effect when tested between 6-100 μM for up to 24 h (data not shown).

Effect of sHA 14-1 on Cellular Ca^{2+} Homeostasis. Although ER-localized anti-apoptotic Bcl-2 family proteins have been demonstrated to inhibit apoptosis by modulating ER calcium storage and release (Giorgi *et al*., 2008; Pinton and Rizzuto, 2006; Kuo *et al*., 1998), the effect of Bcl-2 antagonists on intracellular calcium regulation has been minimally studied (An *et al*., 2004). Analysis of human leukemia cells revealed that sHA 14-1 induced a dose-dependent release of calcium in NALM-6 (Fig. 2A) and JURKAT (Fig. 2B). The well-studied SERCA inhibitor, thapsigargin, rapidly increased cytosolic calcium through the release of ER calcium in NALM-6 (Fig. 2C) and JURKAT (Fig. 2D). The kinetics of increased cytosolic calcium induced by sHA 14-1 was similar to that induced by thapsigargin (Figs. 2E and 2F). Furthermore, addition of thapsigargin following sHA 14-1 resulted in no significant cytosolic calcium increase beyond that induced by sHA 14-1 alone (Figs. 2E and 2F). This lack of additivity implied that both compounds were emptying the same pool of intracellular Ca^{2+}: namely the ER calcium store. The inactive analog of sHA 14-1, isHA 14-1, induced no cytosolic calcium increase (Figs. 2G and 2H). The well-known Bcl-2 antagonist, ABT-737, did not induce significant ER calcium release under the same experimental conditions (data not shown).

Because cytosolic calcium can mediate apoptosis (Szalai *et al.*, 1999; Pinton *et al.*, 2001) and ER-localized Bcl-2 proteins inhibit apoptosis through control of ER calcium release (Scorrano *et al.*, 2003; Thomenious and Distelhorst, 2003; Zong *et al.*, 2003), the cytotoxic effect of sHA 14-1 might be mediated by ER calcium release. To test this possibility, NALM-6 cells were pre-treated with a cell-permeable ester form of EGTA, EGTA-AM, which chelated cytosolic calcium induced by sHA 14-1. Evaluation of cytotoxicity demonstrated that EGTA-AM pre-treatment decreased the cytotoxicity of sHA 14-1 to NALM-6 (Fig. 3A). Considering that EGTA is good for short-term buffering of calcium, it is not surprising that the protective effects of EGTA were small; nevertheless, these results suggest that ER-released calcium is at least partially responsible for the cytotoxicity induced by sHA 14-1.

Targeting the ER to Induce Calcium Release. In order to determine whether sHA 14-1 directly interacts with ER to induce Ca^{2+} release, we examined $^{45}Ca^{2+}$ fluxes in permeabilized NALM-6 cells. These experiments were conducted in the presence of FCCP, a mitochondrial uncoupler (Hutson *et al.*, 1976), to prevent Ca^{2+} uptake into mitochondria. In cells pretreated with sHA 14-1, the extent of ER-localized $^{45}Ca^{2+}$ accumulation was lower than that in control cells (Fig. 3B). Furthermore, in cells loaded to steady state with $^{45}Ca^{2+}$, 2-min sHA 14-1 treatment resulted in a loss of ER Ca^{2+} in a dose-dependent manner (EC_{50} of 4.1 μM, Fig. 3C). As a control, IP_3 effected a more potent depletion (EC_{50} of 106 nM, Fig. 3D). Similar results were obtained using U937 cells (data not shown). Therefore, both experiments

Molecular Pharmacology Fast Forward. Published on June 26, 2009 as DOI: 10.1124/mol.109.055830
This article has not been copyedited and formatted. The final version may differ from this version.

implied that sHA 14-1 caused a dose-dependent loss of Ca^{2+} from the ER via directly targeting ER-localized biomolecule(s).

Inhibition of SERCAs by sHA 14-1. Because IP_3Rs and SERCAs are two major ER-localized calcium regulatory transporters which interact with ER-localized Bcl-2 family proteins to regulate cellular calcium homeostasis (Kuo *et al*., 1998; Dremina *et al*., 2006; Dremina *et al*., 2004; Oakes *et al.*, 2005; Chen *et al*., 2004; Li *et al*., 2002; White *et al*., 2005; Hanson *et al*., 2008; Li *et al*., 2007), sHA 14-1 may induce ER calcium release by modulating either or both of these targets. To determine whether perturbation of the IP_3Rs was responsible for sHA 14-1 induced ER calcium release, we tested the effect of sHA 14-1 on IP_3R *null* DT-40 cells and DT-40 parent cells. These two cell lines were evaluated for their sensitivity to sHA 14-1 based on cytotoxicity and extent of calcium release. As shown in Fig. 4A, sHA 14-1 demonstrated similar cytotoxicity in both cell lines, with the IP_3R *null* line being slightly more sensitive (IP_3R *null* DT-40 was found to be moderately more sensitive to other standard anticancer agents as well, data not shown). Fig. 4B shows that sHA 14-1 also induced the same degree of calcium release in both cell lines. Together, these data suggest that IP_3Rs are unlikely to be the molecular targets responsible for sHA 14-1 induced ER calcium release.

We then explored whether SERCAs might be a target responsible for sHA 14-1 induced ER calcium release. We first tested whether sHA 14-1 may interfere with thapsigargin in ER-calcium release. NALM-6 and JURKAT leukemic cells were co-treated with 100 nM thapsigargin, the minimal concentration to induce full Ca^{2+} release, and increasing concentrations of sHA 14-1. sHA 14-1 indeed antagonized thapsigargin-induced calcium release in a dose-dependent manner (Figs. 5A and B), suggesting that sHA 14-1 may compete with thapsigargin to interact with SERCAs. We next examined the effect of sHA 14-1 on SERCA enzymatic activity using SR membranes purified from rabbit skeletal muscle for SERCA 1A (Fig. 5C) and from pig brain for SERCA 2B (Fig. 5D). The results show that sHA 14-1 demonstrated moderate inhibition of SERCA 1A and 2B with an IC_{50} of 29.2 ± 4.9 μM and 23.5 ± 4.2 μM, respectively. Lastly, since SERCA has been reported to be regulated by Bcl-2 (Dremina *et al*., 2006; Dremina *et al*., 2004; Kuo *et al*., 1998), we considered it possible that sHA 14-1 may modulate SERCA function through antagonizing Bcl-2 protein. Because only 75% of the proteins from the samples used in Figs. 5A-D were SERCAs, we prepared samples with >99% proteins being SERCAs and sHA 14-1 demonstrated similar inhibitory activity (data not shown). Fig. 5E shows a Coomassie Blue stain and Western blot of this 99% purified SERCA sample, which detected no Bcl-2 proteins (no Bcl-X_L or MCL-1 proteins as well based on Western analyses, data not shown). As a control we electrophoresed decreasing concentrations of NALM-6 total protein lysate, and Bcl-2 was easily detected when as little as 0.2 μg of protein was blotted (Fig. 5E). These results suggest that SERCAs are likely to be directly antagonized by sHA 14-1, resulting in an increase in cytosolic calcium and depletion of ER calcium storage.

Molecular Pharmacology Fast Forward. Published on June 26, 2009 as DOI: 10.1124/mol.109.055830
This article has not been copyedited and formatted. The final version may differ from this version.

sHA 14-1 Induced ER and Mitochondrial Stress. Given the effect of sHA 14-1 on ER calcium release (Fig. 2), we next examined whether it would induce ER stress. Expression of the ER stress-associated transcription factor ATF4/CREB-2, one of the characteristics of an ER stress response, was therefore evaluated by Western blotting. Exposure of NALM-6 to 50 μM sHA 14-1 led to induction of ATF4 between 30 and 60 min (Fig. 6A), and a dose response analysis indicated increasing induction from 25-100 μM of sHA 14-1 (Fig. 6B). Incubation of NALM-6 with thapsigargin served as a positive control. In order to compare the mechanism of action of sHA 14-1 to ABT-737, we used the RS4;11 human leukemic cell line, which had previously been shown to be highly sensitive to ABT-737 (Del Gaizo Moore *et al.*, 2008). As shown in Fig. 6C, ATF4 was induced by sHA 14-1 but not ABT-737. Thapsigargin served as a positive control and isHA 14-1 served as a negative control for ATF4 induction (Fig. 6C).

The effects of sHA 14-1 on $\Delta\psi$m and cytochrome *c* release were evaluated by flow cytometry. Preliminary experiments revealed that loss of $\Delta\psi$m was not detected until 6 h following addition of sHA 14-1 to NALM-6 (data not shown). As shown in Fig. 7A, exposure of NALM-6 to 50 and 100 μM sHA 14-1 for 8 h induced a loss of $\Delta\psi$m based on reduction in TMRE staining intensity. Cells treated with identical concentrations of the inactive variant isHA 14-1 did not undergo changes in $\Delta\psi$m. ABT-737 also induced a loss of $\Delta\psi$m (Fig. 7A), which was detectable as early as 2 h (data not shown). As expected based on its well-characterized mechanism of action as a BH3 mimetic (Oltersdorf *et al*., 2005; Del Gaizo Moore *et al*., 2008), ABT-737 rapidly induced cytochrome *c* release. However, incubation of NALM-6 for 8 h with sHA 14-1 did not induce detectable cytochrome *c* release (Fig. 7A). The different effect of sHA 14-1 and ABT-737 on cytochrome *c* release was not unique to NALM-6, since analysis of RS4;11 yielded comparable results (Fig. 7B). The failure of sHA 14-1 to induce a loss of cytochrome *c* could not be explained by kinetics, since analysis at earlier (2-4 h) and later (10-14 h) time points gave the same results (data not shown).

Since thapsigargin and sHA 14-1 exerted similar effects on ER calcium release (Fig. 2) and ER stress (Fig. 6), we assessed whether thapsigargin would induce a loss of $\Delta\psi$m similar to sHA 14-1. The results in Fig. 7C show that 0.1 and 1 μM thapsigargin had no effect on $\Delta\psi$m after 6 h incubation with NALM-6 or RS4;11, and only a very subtle effect on RS4;11 (< 10% of cells) at 24 h. Other experiments tested thapsigargin at concentrations ranging from 0.1 nM to 1 μM for 2-48 h. At no time and at no concentration did we detect a reduction in $\Delta\psi$m similar to that exerted by sHA 14-1 and ABT-737 (data not shown). Thus, despite their similar capacity to induce ER calcium release and ATF4, sHA 14-1 and thapsigargin exert different effects on $\Delta\psi$m.

Although we could not detect sHA 14-1 induced cytochrome *c* release by flow cytometry (Fig. 7A), this may have been due to assay sensitivity (Tian *et al*., 2008). We therefore assessed caspase-9 activation as a surrogate outcome of mitochondrial damage and cytochrome *c* release. Fig. 6C shows that incubation of

Molecular Pharmacology Fast Forward. Published on June 26, 2009 as DOI: 10.1124/mol.109.055830
This article has not been copyedited and formatted. The final version may differ from this version.

RS4;11 with sHA 14-1 for 2 h resulted in a detectable caspase-9 cleavage product at 100 μM. In contrast, thapsigargin and the inactive variant of sHA 14-1 did not induce cleavage of caspase-9. As expected, ABT-737 induced robust cleavage of caspase-9, as did HA 14-1. These collective results suggest a primary targeting effect of ABT-737 and thapsigargin on the mitochondria and ER, respectively, and a dual mode of action of sHA 14-1.

Given the minimal effect of sHA 14-1 on loss of mitochondrial cytochrome c (Fig. 7) and activation of caspase-9 (Fig. 6C), we assessed the relative degree of caspase dependency using the pan-caspase inhibitor Z-VAD-fmk. RS4;11 cells were incubated overnight with sHA 14-1 in the absence or presence of Z-VAD-fmk, and cell survival/apoptosis was assessed by PI/Annexin V staining. The results show that incubation with DMSO, the inactive compound isHA 14-1, Z-VAD-fmk by itself, or TG had no effect on RS4;11 cells based on light scatter characteristics and PI/Annexin V staining (Fig. 8). Incubation with ABT-737 gave the expected increase in Annexin V+/PI- and Annexin V+/PI+ events compared to the DMSO control. Also evident is that the majority of ABT-737 treated cells underwent a uniform decrease in cell size; as shown by a decrease in forward light scatter characteristics (note events encircled by dashed line). This is the prototypical change that occurs in cells undergoing apoptosis through the mitochondrial pathway. As expected, inclusion of Z-VAD-fmk reduced the frequency of Annexin V+/PI- events in ABT-737 treated cells from 31% to 11%, and a concomitant increase (18% to 66%) in cells with viable light scatter characteristics. In contrast, inclusion of Z-VAD-fmk in sHA 14-1 treated cells had no effect on the percentage of Annexin V+/PI- events, and a modest effect on the percentage of cells with viable light scatter characteristics (11% to 21%). Of note is the profound difference in the overall light scatter characteristics of sHA 14-1 and ABT-737 treated cells, with the former exhibiting a much greater degree of side scatter heterogeneity than the latter.

Discussion

Rational drug design that targets anti-apoptotic Bcl-2 family members is a promising approach to treating cancer (Letai, 2008). Despite the proven efficacy of compromising Bcl-2 function and unleashing the pro-apoptotic activity of BAX/BAK and BH-3 only proteins, the intracellular events that culminate in the demise of tumor cells may differ depending on the antagonist. HA 14-1 is an organic compound originally discovered by computer modeling that predicted binding to Bcl-2 (Wang *et al*., 2000). It has been reported to synergize with a variety of anti-cancer agents to promote apoptosis in hematopoietic and solid tumors (Pei *et al*., 2003; Sinicrope *et al*., 2004; Nimmanapalli *et al*., 2003; Pei *et al*., 2004; Sinicrope and Penington, 2005; Milella *et al*., 2004; Manero *et al*., 2006; Niizuma *et al*., 2006; Milella *et al*., 2002; An *et al*., 2007; Lickliter *et al*., 2007). However, we have previously demonstrated that HA 14-1 is highly unstable when incubated in standard tissue culture conditions and has a half-life of ~ 15 min

Molecular Pharmacology Fast Forward. Published on June 26, 2009 as DOI: 10.1124/mol.109.055830
This article has not been copyedited and formatted. The final version may differ from this version.

(Doshi *et al*., 2007). Of additional concern was the observation that HA 14-1 decomposes to generate reactive oxygen species (ROS), which have potent pro-apoptotic activity (Doshi *et al*., 2007). Thus, many prior published studies of HA 14-1 activity may have been measuring the consequences of ROS on cell viability/apoptotic fate, in lieu of or in addition to its effect of antagonizing anti-apoptotic Bcl-2 family proteins. Synthesis of the more stable analog sHA 14-1 alleviated the decomposition problem, and generation of ROS was negligible (Tian *et al*., 2008). The goal of the current study was to elucidate the mechanism(s) underlying the pro-apoptotic activity of sHA 14-1.

Since anti-apoptotic Bcl-2 family proteins can localize to the ER and regulate apoptosis through calcium homeostasis, small-molecule antagonists can potentially affect cellular calcium homeostasis. We found that sHA 14-1 rapidly induced an increase in cytosolic calcium through release of ER calcium storage in a dose-dependent manner (Figs 2A and 2B). We further demonstrated that sHA 14-1 induced the release of an ER calcium storage pool indistinguishable from the potent SERCA inhibitor thapsigargin, since addition of thapsigargin following sHA 14-1treatment induced no further calcium release (Figs. 2E and 2F). Although the intensity of calcium release induced by sHA 14-1 was not as pronounced as thapsigargin, the kinetics was similar (Figs. 2C-F). The cytosolic calcium increase was at least partially responsible for the cytotoxicity of sHA 14-1 since its chelation resulted in protection of cells against sHA 14-1 (Fig. 3A). The partial protection through chelation is likely due to the incomplete suppression of cytosolic calcium increase. In addition, the ER calcium depletion may function as a cytotoxic signal that can not be affected by cytosolic calcium chelation (Boelens *et al.*, 2007).

The results in Figs. 2 and 3A did not clarify whether the cellular target of sHA 14-1 responsible for ER calcium release localized to the ER. However, disruption of mitochondrial function using FCCP, a mitochondria uncoupling agent, revealed that sHA 14-1 was still capable of reducing ER calcium storage in permeabilized NALM-6 and U937 leukemic cells (Fig. 3B-D). These results suggest that at least one of the molecular targets of sHA 14-1 localizes to the ER.

There are several transporters that control ER calcium homeostasis, including IP_3Rs and SERCAs. Both have been reported to be regulated by Bcl-2 family proteins (Kuo *et al*., 1998; Dremina *et al*., 2006; Dremina *et al*., 2004; Oakes *et al*., 2005; Chen *et al*., 2004; Li *et al*., 2002; White *et al*., 2005; Hanson *et al*., 2008; Li *et al*., 2007). We used DT-40 and IP_3R *null* DT-40 cells to determine the potential role of IP_3Rs in sHA 14-1 induced calcium release. The results in Fig. 4 showed that an absence of IP_3Rs did not alter the sensitivity of DT-40 cells to the cytotoxic effect of sHA 14-1 and sHA 14-1-induced ER calcium release. These results suggest that IP_3Rs are unlikely to be directly targeted by sHA 14-1.

Despite the fact that sHA 14-1 is an antagonist of Bcl-2 and Bcl-X_L with increased binding potency compared to HA 14-1 (Tian *et al*., 2008), we were surprised to discover that sHA 14-1 partially blocked thapsigargin-induced ER calcium release in a dose-dependent manner (Figs. 5A and 5B). This result

Molecular Pharmacology Fast Forward. Published on June 26, 2009 as DOI: 10.1124/mol.109.055830
This article has not been copyedited and formatted. The final version may differ from this version.

suggests that sHA 14-1 may induce ER calcium release through the SERCA pathway. This was confirmed by showing that sHA 14-1 inhibited the activity of both SERCA1A and 2B (Figs. 5C and 5D). Although Bcl-2 has been reported to regulate the function of SERCAs (Kuo *et al*., 1998; Dremina *et al*., 2006; Dremina *et al*., 2004), our studies suggest that sHA 14-1 probably directly antagonizes SERCAs to induce ER calcium release since no Bcl-2 protein was detected in the SERCA samples (Fig. 5E). The paradoxical capability of sHA 14-1 to suppress thapsigargin-induced ER calcium release (Figs. 5A and 5B) is likely because thapsigargin has a higher intrinsic activity to induce ER calcium release through SERCAs, while sHA 14-1 has a lower intrinsic activity. In addition to the effects on ER calcium and SERCA activity, sHA 14-1 treatment led to induction of ATF4 (Fig. 6). Thus, sHA 14-1 has a functional effect on the ER similar to thapsigargin, with a rapid release of ER calcium followed by subsequent ATF4 induction.

sHA 14-1 induced a loss of $\Delta\psi m$ (Fig. 7A) and caspase-9 activation (Fig. 6C) in leukemic cell lines 2-6 h after treatment. Its inactive counterpart, isHA 14-1, failed to induce a loss of $\Delta\psi m$ and caspase-9 activation under the same conditions, while ABT-737 induced a much more prominent loss of $\Delta\psi m$ (Fig. 7A) and caspase-9 activation (Fig. 6C). It remains to be determined whether there are ER/mitochondrial communications in response to sHA 14-1 induced stress or whether these are two independent processes.

The parent compound HA 14-1 has been reported to impact ER and mitochondrial function (An *et al*., 2004). However, those results might be attributable to the production of ROS following the rapid decomposition of HA 14-1 (Doshi *et al*., 2007; Zhang *et al.*, 2006). In our own studies of HA 14-1, we noted effects on $\Delta\psi m$ and caspase-9 activation within 1-2 h after treatment (data not shown), whereas comparable effects by sHA 14-1 required 6-8 h (Fig. 7). The slower kinetics of cell death, the paucity of mitochondrial outer membrane permeabilization, the weak caspase-9 activation, and the relative insensitivity to the pan-caspase inhibitor Z-VAD-fmk, are all consistent with a caspase independent mechanism of cell death induced by sHA 14-1 (Tait *et al.*, 2008). The prominent change in the light scatter characteristics of sHA 14-1 treated cells (Fig. 8) is suggestive of subcellular vacuole accumulation, and we are currently investigating whether this includes an autophagic component.

In conclusion, the current study shows that a small-molecule antagonist of anti-apoptotic Bcl-2 family proteins, sHA 14-1, can exhibit subcellular targeting effects that encompass two vulnerable sites for initiation of apoptosis. Our collective data suggest a model wherein sHA 14-1 targets SERCAs in ER with a higher potency than the anti-apoptotic Bcl-2 family proteins in the mitochondria. This model is supported by the rapid induction of ER calcium loss (Fig 2) and the subsequent induction of ATF4 (Fig. 6). An effect on mitochondrial function is not detectable until 6-8 h after sHA 14-1 treatment (Fig. 7). The mechanism of the pro-apoptotic effect of sHA 14-1 is therefore distinct from ABT-737, which primarily initiates apoptosis by targeting the mitochondria, and thapsigargin, which acts specifically at the ER. The capacity of a small molecule such as sHA 14-1 to bind multiple intracellular targets may be an attractive

Molecular Pharmacology Fast Forward. Published on June 26, 2009 as DOI: 10.1124/mol.109.055830
This article has not been copyedited and formatted. The final version may differ from this version.

strategy to overcome drug resistance that emerges as a consequence of multi-gene mutations (Frantz, 2005).

Acknowledgements

We thank Dr. Chi Li (University of Louisville) for providing DT-40 B lymphoma cell line and IP_3R *null* DT-40 cell line. We also thank Trinh Nguyen for technical assistance.

Molecular Pharmacology Fast Forward. Published on June 26, 2009 as DOI: 10.1124/mol.109.055830
This article has not been copyedited and formatted. The final version may differ from this version.

References

Adams JM and Cory S (2007) The Bcl-2 apoptotic switch in cancer development and therapy. *Oncogene* **26**: 1324-1337.

An J, Chen Y and Huang Z (2004) Critical Upstream Signals of Cytochrome c Release Induced by a Novel Bcl-2 Inhibitor. *J. Biol. Chem.* **279**: 19133-19140.

An J, Chervin A S, Nie A, Ducoff H S and Huang Z (2007) Overcoming the radioresistance of prostate cancer cells with a novel Bcl-2 inhibitor. *Oncogene* **26**: 652-661.

Bilmen JG and Michelangeli F (2002) Inhibition of the type 1 inositol 1,4,5-trisphosphate receptor by 2-aminoethoxydiphenylborate. *Cell Signal.* **14**: 955-960.

Birmachu W, Nisswandt F L and Thomas D D (1989) Conformational transitions in the calcium adenosinetriphosphatase studied by time-resolved fluorescence resonance energy transfer. *Biochemistry* **28**: 3940-3947.

Boelens J, Lust S, Offner F, Bracke M E and Vanhoecke B W (2007) The endoplasmic reticulum: a target for new anticancer drugs. *in vivo* **21**: 215-226.

Bollig A, Xu L, Thakur A, Wu J, Kuo T H and Liao J D (2007) Regulation of intracellular calcium release and PP1alpha in a mechanism for 4-hydroxytamoxifen-induced cytotoxicity. *Mol. Cell Biochem.* **305**: 45-54.

Breckenridge DG, Germain M, Mathai J P, Nguyen M and Shore G C (2003) Regulation of apoptosis by endoplasmic reticulum pathways. *Oncogene* **22**: 8608-8618.

Chen R, Valencia I, Zhong F, McColl K S, Roderick H L, Bootman M D, Berridge M J, Conway S J, Holmes A B, Mignery G A, Velez P and Distelhorst C W (2004) Bcl-2 functionally interacts with inositol 1,4,5-trisphosphate receptors to regulate calcium release from the ER in response to inositol 1,4,5-trisphosphate. *J. Cell Biol.* **166**: 193-203.

Dai Y, Rahmani M, Corey S J, Dent P and Grant S (2004) A Bcr/Abl-independent, Lyn-dependent Form of Imatinib Mesylate (STI-571) Resistance Is Associated with Altered Expression of Bcl-2. *J. Biol. Chem.* **279**: 34227-34239.

Del Gaizo Moore V, Schlis K D, Sallan S E, Armstrong S A and Letai A (2008) Bcl-2 dependence and ABT-737 sensitivity in acute lymphoblastic leukemia. *Blood* **111**: 2300-2309.

Denmeade SR and Isaacs J T (2005) The SERCA pump as a therapeutic target: making a "smart bomb" for prostate cancer. *Cancer Biol. Ther.* **4**: 14-22.

Doshi JM, Tian D and Xing C (2007) Ethyl-2-amino-6-bromo-4-(1-cyano-2-ethoxy-2-oxoethyl)-4*H*-chromene-3-carboxylate (HA 14-1), a prototype small-molecule antagonist against anti-apoptotic Bcl-2 proteins, decomposes to generate reactive oxygen species (ROS) that induce apoptosis. *Mol. Pharm.* **4**: 919-928.

Doshi JM and Xing C (2008) Antagonists against anti-apoptotic Bcl-2 family proteins for cancer treatment. *Mini. Rev. Org. Chem.* **5**: 171-178.

Dremina ES, Sharov V S, Kumar K, Zaidi A, Michaelis E K and Schöneich C (2004) Anti-apoptotic protein Bcl-2 interacts with and destabilizes the sarcoplasmic/endoplasmic reticulum Ca2+-ATPase (SERCA). *Biochem. J.* **383**: 361-370.

Dremina ES, Sharov V S and Schöneich C (2006) Displacement of SERCA from SR lipid caveolae-related domains by Bcl-2: a possible mechanism for SERCA inactivation. *Biochemistry* **45**: 175-184.

Fernandez JL, Rosemblatt M and Hidalgo C (1980) Highly purified sarcoplasmic reticulum vesicles are devoid of Ca2+-independent ('basal') ATPase activity. *Biochim. Biophys. Acta.* **599**: 552-568.

Frantz S (2005) Drug discovery: playing dirty. *Nature* **437**: 942-943.

Giorgi C, Romagnoli A, Pinton P and Rizzuto R (2008) Ca2+ signaling, mitochondria and cell death. *Curr. Mol. Med.* **8**: 119-130.

Hanson CJ, Bootman M D, Distelhorst C W, Wojcikiewicz R J and Roderick H L (2008) Bcl-2 suppresses Ca(2+) release through inositol 1,4,5-trisphosphate receptors and inhibits Ca(2+) uptake by mitochondria without affecting ER calcium store content. *Cell Calcium* **44**: 324-338.

Hurwitz R, Hozier J, LeBien T, Minowada J, Gajl-Peczalska K, Kubonishi I and Kersey J (1979) Characterization of a leukemic cell line of the pre-B phenotype. *Int. J. Cancer*. **23**: 174-180.

Hutson SM, Pfeiffer D R and Lardy H A (1976) Effect of cations and anions on the steady state kinetics of energy-dependent Ca2+ transport in rat liver mitochondria. *J. Biol. Chem.* **251**: 5251-5258.

Krajewski S, Tanaka S, Takayama S, Schibler M J, Fenton W and Reed J C (1993) Investigation of the subcellular distribution of the bcl-2 oncoprotein: residence in the nuclear envelope, endoplasmic reticulum, and outer mitochondrial membranes. *Cancer Res.* **53**: 4701-4714.

Kuo TH, Kim H R, Zhu L, Yu Y, Lin H M and Tsang W (1998) Modulation of endoplasmic reticulum calcium pump by Bcl-2. *Oncogene* **17**: 1903-1910.

Lee DI, Sumbilla C, Lee M, Natesavelalar C, Klein M G, Ross D D, Inesi G and Hussain A (2007) Mechanisms of resistance and adaptation to thapsigargin in androgen-independent prostate cancer PC3 and DU145. *Arch. Biochem. Biophys.* **464**: 19-27.

Letai A (2005) Pharmacological manipulation of Bcl-2 family members to control cell death. *J. Clin. Invest.* **115**: 2648-2655.

Letai AG (2008) Diagnosing and exploiting cancer's addiction to blocks in apoptosis. *Nat. Rev. Cancer*. **8**: 121-132.

Li C, Fox C J, Master S R, Bindokas V P, Chodosh L A and Thompson C B (2002) Bcl-X(L) affects Ca(2+) homeostasis by altering expression of inositol 1,4,5-trisphosphate receptors. *Proc. Natl. Acad. Sci. U. S. A.* **99**: 9830-9835.

Li C, Wang X, Vais H, Thompson C B, Foskett J K and White C (2007) Apoptosis regulation by Bcl-x(L) modulation of mammalian inositol 1,4,5-trisphosphate receptor channel isoform gating. *Proc. Natl. Acad. Sci. U. S. A.* **104**: 12565-12570.

Lickliter JD, Cox J, McCarron J, Martinex N R, Schmidt C W, Lin H, Nieda M and Nicol A J (2007) Small-molecule Bcl-2 inhibitors sensitise tumor cells to immune-mediated destruction. *Br. J. Cancer* **96**: 600-608.

Lickliter JD, Wood N J, Johnson L, McHugh G, Tan J, Wood F, Cox J and Wickham N W (2003) HA14-1 selectively induces apoptosis in Bcl-2-overexpressing leukemia/lymphoma cells, and enhances cytarabine-induced cell death. *Leukemia* **17**: 2074-2080.

Liu X, Lee K and Herbison A E (2008) Kisspeptin excites gonadotropin-releasing hormone neurons through a phospholipase C/calcium-dependent pathway regulating multiple ion channels. *Endocrinology* **149**: 4605-4614.

Manero F, Gautier F, Gallenne T, Cauquil N, Grée D, Cartron P-F, Geneste O, Grée R, Vallette F M and Juin P (2006) The Small Organic Compound HA14-1 Prevents Bcl-2 Interaction with Bax to Sensitize Malignant Glioma Cells to Induction of Cell Death. *Cancer Res.* **66**: 2757-2764.

Michelangeli F and Munkonge F M (1991) Methods of reconstitution of the purified sarcoplasmic reticulum (Ca(2+)-Mg2+)-ATPase using bile salt detergents to form membranes of defined lipid to protein ratios or sealed vesicles. *Anal. Biochem.* **194**: 231-236.

Milella M, Estrov Z, Kornblau S M, Carter B Z, Konopleva M, Tari A, Schober W D, Harris D, Leysath C E, Lopez-Berestein G, Huang Z and Andreeff M (2002) Synergistic induction of apoptosis by simultaneous disruption of the Bcl-2 and MEK/MAPK pathways in acute myelogenous leukemia. *Blood* **99**: 3461-3464.

Milella M, Trisciuoglio D, Bruno T, Ciuffreda L, Mottolese M, Cianciulli A, Cognetti F, Zangemeister-Wittke U, Del Bufalo D and Zupi G (2004) Trastuzumab Down-Regulates Bcl-2 Expression and Potentiates Apoptosis Induction by Bcl-2/Bcl-XL Bispecific Antisense Oligonucleotides in HER-2Gene-Amplified Breast Cancer Cells. *Clin. Cancer Res.* **10**: 7747-7756.

Niizuma H, Nakamura Y, Ozaki T, Nakanishi H, Ohira M, Isogai E, Kageyama H, Imaizumi M and Nakagawara A (2006) Bcl-2 is a key regulator for the retinoic acid-induced apoptotic cell death in neuroblastoma. *Oncogene* **25**: 5046-5055.

Nimmanapalli R, O'Bryan E, Kuhn D, Yamaguchi H, Wang H and Bhalla K N (2003) Regulation of 17-AAG--induced apoptosis: role of Bcl-2, Bcl-xL, and Bax downstream of 17-AAG--mediated down-regulation of Akt, Raf-1, and Src kinases. *Blood* **102**: 269-275.

O'Neill JP, Velalar C N, Lee D I, Zhang B, Nakanishi T, Tang Y, Selaru F, Ross D, Meltzer S J and Hussain A (2006) Thapsigargin resistance in human prostate cancer cells. *Cancer* **107**: 649-659.

Oakes SA, Scorrano L, Opferman J T, Bassik M C, Nishino M, Pozzan T and Korsmeyer S J (2005) Proapoptotic BAX and BAK regulate the type 1 inositol trisphosphate receptor and calcium leak from the endoplasmic reticulum. *Proc. Natl. Acad. Sci.* **102**: 105-110.

Oltersdorf T, Elmore S W, Shoemaker A R, Armstrong R C, Augeri D J, Belli B A, Bruncko M, Deckwerth T L, Dinges J, Hajduk P J, Joseph M K, Kitada S, Korsmeyer S J, Kunzer A R, Letai A, Li C, Mitten M J, Nettesheim D J, Ng S, Nimmer P M, O'Connor J M, Oleksijew A, Petros A M, Reed J C, Shen W, Tahir S K, Thompson C B, Tomaselli K J, Wang B, Wendt M B, Zhang H, Fesik S W and Rosenberg S H (2005) An inhibitor of Bcl-2 family proteins induces regression of solid tumours. *Nature* **435**: 677-681.

Ow YL, Green D R, Hao Z and Mak T W (2008) Cytochrome c: functions beyond respiration. *Nat. Rev. Mol. Cell Biol.* **9**: 532-42.

Pei X, Dai Y and Grant S (2003) The proteasome inhibitor bortezomib promotes mitochondrial injury and apoptosis induced by the small molecule Bcl-2 inhibitor HA14-1 in multiple myeloma cells. *Leukemia* **17**: 2036-2045.

Pei X, Dai Y and Grant S (2004) The small-molecule Bcl-2 inhibitor HA14-1 interacts synergistically with flavopiridol to induce mitochondrial injury and apoptosis in human myeloma cells through a free radical-dependent and Jun NH2-terminal kinase-dependent mechanism. *Mol. Cancer Ther.* **3**: 1513-1524.

Pinton P, Ferrari D, Rapizzi E, Di Virgilio F, Pozzan T and Rizzuto R (2001) The Ca^{2+} concentration of the endoplasmic reticulum is a key determinant of ceramide-induced apoptosis: significance for the molecular mechanism of Bcl-2 action. *EMBO J.* **20**: 2690-2701.

Pinton P and Rizzuto R (2006) Bcl-2 and Ca2+ homeostasis in the endoplasmic reticulum. *Cell Death Differ.* **13**: 1409-1418.

Reddy LG, Cornea R L, Winters D L, McKenna E and Thomas D D (2003) Defining the molecular components of calcium transport regulation in a reconstituted membrane system. *Biochemistry* **42**: 4585-4592.

Reed JC (2003) Apoptosis-targeted therapies for cancer. *Cancer Cell* **3**: 17-22.

Reed JC (2008) Bcl-2-family proteins and hematologic malignancies: history and future prospects. *Blood* **111**: 3322-3330.

Molecular Pharmacology Fast Forward. Published on June 26, 2009 as DOI: 10.1124/mol.109.055830
This article has not been copyedited and formatted. The final version may differ from this version.

Rong Y and Distelhorst C W (2008) Bcl-2 protein family members: versatile regulators of calcium signaling in cell survival and apoptosis. *Annu. Rev. Physiol.* **70**: 73-91.

Scorrano L, Oakes S A, Opferman J T, Cheng E H, Sorcinelli M D, Pozzan T and Korsmeyer S J (2003) BAX and BAK regulation of endoplasmic reticulum Ca2+: a control point for apoptosis. *Science* **300**: 135-139.

Shah N, Asch R J, Lysholm A S and LeBien T W (2004) Enhancement of stress-induced apoptosis in B-lineage cells by caspase-9 inhibitor. *Blood* **104**: 2873-2878.

Sinicrope FA, Penington R C and Tang X M (2004) Tumor Necrosis Factor-Related Apoptosis-Inducing Ligand-Induced Apoptosis Is Inhibited by Bcl-2 but Restored by the Small Molecule Bcl-2 Inhibitor, HA 14-1, in Human Colon Cancer Cells. *Clin. Cancer Res.* **10**: 8284-8292.

Sinicrope SA and Penington R C (2005) Sulindac sulfide-induced apoptosis is enhanced by a small-molecule Bcl-2 inhibitor and by TRAIL in human colon cancer cells overexpressing Bcl-2. *Mol. Cancer Ther*. **4**: 1475-1483.

Stong RC, Korsmeyer S J, Parkin J L, Arthur D C and Kersey J H (1985) Human acute leukemia cell line with the t(4;11) chromosomal rearrangement exhibits B lineage and monocytic characteristics. *Blood* **65**: 21-31.

Sugawara H, Kurosaki M, Takata M and Kurosaki T (1997) Genetic evidence for involvement of type 1, type 2 and type 3 inositol 1,4,5-trisphosphate receptors in signal transduction through the B-cell antigen receptor. *EMBO J.* **16**: 3078-88.

Szalai G, Krishnamurthy R and Hajnoczky G (1999) Apoptosis driven by IP(3)-linked mitochondrial calcium signals. *EMBO J.* **18**: 6349-6361.

Tait SWG and Green DR (2008) Caspase-independent death; leaving the set without the final cut. *Oncogene* 27: 6452-6461.

Thomenious MJ and Distelhorst C W (2003) Bcl-2 on the endoplasmic reticulum: protecting the mitochondria from a distance. *J. Cell Sci.* **116**: 4493-4499.

Tian D, Das S, Doshi J M, Peng J, Lin J and Xing C (2008) sHA 14-1, a stable and ROS-free antagonist against anti-apoptotic Bcl-2 proteins, bypasses drug resistances and synergizes cancer therapies in human leukemia cell. *Cancer Lett.* **259**: 198-208.

Wang J, Liu D, Zhang Z, Shan S, Han X, Srinivasula S M, Croce C M, Alnemri E S and Huang Z (2000) Structure-based discovery of an organic compound that binds Bcl-2 protein and induces apoptosis of tumor cells. *Proc. Natl. Acad. Sci.* **97**: 7124-7129.

White C, Li C, Yang J, Petrenko N B, Madesh M, Thompson C B and Foskett J K (2005) The endoplasmic reticulum gateway to apoptosis by Bcl-X(L) modulation of the InsP3R. *Nat. Cell Biol.* **7**: 1021-1028.

Wootton LL and Michelangeli F (2006) The effects of the phenylalanine 256 to valine mutation on the sensitivity of sarcoplasmic/endoplasmic reticulum Ca2+ ATPase (SERCA) Ca2+ pump isoforms 1, 2, and 3 to thapsigargin and other inhibitors. *J. Biol. Chem.* **281**: 6970-6976.

Wörmann B, Anderson J M, Liberty J A, Gajl-Peczalska K, Brunning R D, Silberman T L, Arthur D C and LeBien T W (1989) Establishment of a leukemic cell model for studying human pre-B to B cell differentiation. *J. Immunol.* **142**: 110-117.

Xu C, Bailly-Maitre B and Reed J C (2005) Endoplasmic reticulum stress: cell life and death decisions. *J. Clin. Invest.* **115**: 2656-2664.

Zhang Y, Soboloff J, Zhu Z and Berger S A (2006) Inhibition of Ca2+ influx is required for mitochondrial reactive oxygen species-induced endoplasmic reticulum Ca2+ depletion and cell death in leukemia

cells. *Mol. Pharmacol.* **70**: 1424-1434.

Zong WX, Li C, Hatzivassiliou G, Lindsten T, Yu Q C, Yuan J and Thompson C B (2003) Bax and Bak can localize to the endoplasmic reticulum to initiate apoptosis. *J. Cell Biol.* **162**: 59-69.

Molecular Pharmacology Fast Forward. Published on June 26, 2009 as DOI: 10.1124/mol.109.055830
This article has not been copyedited and formatted. The final version may differ from this version.

Footnote:

* This work was supported by NIH grant R01 CA114294, the American Association of College of Pharmacy, and the Leukemia Research Fund, Masonic Cancer Center- University of Minnesota. DH and SNA contributed equally to this work and are co-first authors. TWL and CX contributed equally to this work and are co-senior authors.

Molecular Pharmacology Fast Forward. Published on June 26, 2009 as DOI: 10.1124/mol.109.055830
This article has not been copyedited and formatted. The final version may differ from this version.

Figure legends

Figure 1. Structure of the compounds used in the present study and IC_{50} data for sHA 14-1. (A) Chemical structure of sHA 14-1, isHA 14-1, ABT-737, thapsigargin, and HA 14-1. As described in the Materials and Methods, isHA 14-1 is an inactive variant of sHA 14-1. (B) RS4;11, BLIN-1 and NALM-6 were incubated with various concentrations of sHA 14-1 for 18 h, and Annexin V-/PI- viable cells were quantified by flow cytometry. Each condition represents the mean +/- SD of triplicate values. The results are representative of multiple experiments.

Figure 2. sHA 14-1 induces ER calcium release. NALM-6 (A, C, E, G) and JURKAT (B, D, F, H) were pre-loaded with Fura-2-AM for 30 min. The cells were then washed and fluorescent changes at 340 nM and 380 nM excitation wavelengths were monitored on a dual wavelength fluorometer. Data in A) and B) show the relative extent of cytosolic [Ca^{2+}] changes following a 10-min incubation with the indicated concentrations of sHA 14-1 **(**normalized to the maximum cytosolic [Ca^{2+}] increase induced by sHA 14-1 treatment). Data are mean +/- SD (n = 3 for each conditions). Data in C-H show real time changes in cytosolic [Ca^{2+}] in cells treated with DMSO, 1 μM thapsigargin, 100 μM sHA 14-1, or 100 μM isHA 14-1. The grey tracings indicate that thapsigargin was added 10 min following the initial addition of DMSO (C, D), sHA 14-1 (E, F), or isHA 14-1 (G, H). The results are representative of three separate experiments.

Figure 3. Cytosolic [Ca^{2+}] is an essential factor for sHA 14-1 induced cytotoxicity and sHA 14-1 directly targets the ER. **(A)** Untreated NALM-6 cells (black solid bar) or cells pre-treated for 30 min with 5 μM EGTA-AM (grey bar) were incubated with the indicated concentrations of sHA 14-1. Relative cell viability was determined at 24 h by the Cell TiterBlue cytotoxicity assay. Data are mean +/- SD (n = 3 for each condition). Results are representative of three separate experiments. **: $p < 0.01$; ***: $p < 0.0001$. **(**B**)** Time course of Ca^{2+} uptake into intracellular Ca^{2+} stores in control cells (black solid line, ■) and cells pretreated (5 min) with sHA 14-1 (50 μM, grey dash line, ▲). Data are expressed relative to the final time point intracellular Ca^{2+} content. (C & D) Ca^{2+} release from permeabilized NALM-6 cells loaded to steady state with $^{45}Ca^{2+}$ induced by various concentrations of (C) sHA 14-1 or (D) IP_3. Data are expressed relative to the zero time point before addition of ATP. Data are mean +/- SD (n = 3 for each conditions). The results are representative of two separate experiments.

Molecular Pharmacology Fast Forward. Published on June 26, 2009 as DOI: 10.1124/mol.109.055830
This article has not been copyedited and formatted. The final version may differ from this version.

Figure 4. sHA 14-1 does not disrupt the function of the endoplasmic reticulum IP_3R. (A) Parental (black bar) and IP_3R deficient (grey bar) DT-40 chicken lymphoma cells were incubated with the indicated concentrations of sHA 14-1, and relative cell viability was determined after 24 h by the Cell TiterBlue cytotoxicity assay. (B) Parental (black column) and IP_3R deficient (grey column) DT-40 chicken lymphoma cells were pre-loaded with Fura-2-AM and treated with sHA 14-1 at indicated concentrations. Relative calcium release was measured using the same methods detailed in the Fig. 2 legend and normalized to the amount of calcium release by thapsigarin in parental cells at the concentration of 1 μM. Data are mean +/- SD (n = 3 for each conditions). None of the difference in calcium release between parental and IP_3R deficient cells is statistically significant ($P > 0.05$). The results are representative of three separate experiments.

Figure 5. sHA 14-1 inhibits SERCA enzymatic activity. NALM-6 (A) and JURKAT (B) cells were pre-loaded with Fura-2-AM as described in the Fig. 2 legend. The cells were then incubated with 100 nM thapsigargin (+), the minimal concentration to induce full Ca^{2+} release, and increasing concentrations of sHA 14-1, as shown in the grid below the figures. Calcium release was quantified as in the Fig. 1 legend. Data are mean +/- SD (n = 3 for each conditions). *: $p < 0.05$ **: $p < 0.01$; ***: $p < 0.0001$ in comparison to the quantify of calcium released by TG alone. (C) Increasing concentrations of sHA 14-1 were incubated for 10 min at 37 °C with SR membrane fractions purified from rabbit skeletal muscle. Rabbit skeletal muscle Ca^{2+} ATPase activity (corresponding to SERCA 1A) was measured using the phosphate liberation assay, as previously described (Wootton and Michelangeli, 2006). Data are mean +/- SD (n = 3 for each conditions). (D) Increasing concentrations of sHA 14-1 were incubated for 10 min at 37 °C with pig brain microsomes. Ca^{2+} ATPase activity in these membranes (corresponding to SERCA 2B) was measured using a phosphate liberation assay, as previously described. Data are mean +/- SD (n = 3 for each conditions). E) A SERCA sample (99%, 20μg) was analyzed for the presence of Bcl-2 protein by western blot with NALM-6 protein lysate (0.2, 1, and 5 μg) as a positive control. The results are representative of three separate experiments.

Figure 6. sHA 14-1 induces ER stress. NALM-6 cells were incubated with 1 μM thapsigargin (TG) or 50 μM sHA 14-1 for the indicated times (A), or with 1 μM thapsigargin and the indicated concentrations of sHA 14-1 for 2 h (B). RS4;11 cells were incubated with the indicated compounds and concentrations for 2 h (C). DMSO (2 h) was used as a negative control. The cells were then lysed and Western blotted for detection of ATF4 and cleaved caspase-9 as described in the Materials and Methods. Beta-tubulin (A, B), or AKT (C) were used as loading controls. The results are representative of three separate experiments.

Molecular Pharmacology Fast Forward. Published on June 26, 2009 as DOI: 10.1124/mol.109.055830
This article has not been copyedited and formatted. The final version may differ from this version.

Figure 7. sHA 14-1 induces loss of mitochondrial transmembrane potential ($\Delta\psi m$) but no detectable cytochrome *c* release by flow cytometry. (A) NALM-6 cells were incubated with sHA 14-1 or isHA 14-1 at 50 μM (dashed line) or 100 μM (solid line), or ABT-737 at 5 μM (dashed line) or 10 μM (solid line) for 8 h. (B) RS4;11 cells were incubated for 8 h with 50 μM (dashed line) or 100 μM (solid line) sHA 14-1, or for 2 h with 0.3 μM (dashed line) or 1 μM (solid line) ABT-737. (C) NALM-6 and RS4;11 cells were incubated with 0.1 μM (dashed line) or 1 μM (solid line) thapsigargin for 6 or 24 h. Cells were stained with TMRE or anti-cytochrome *c* and analyzed by flow cytometry. The gray shaded histograms show TMRE staining intensity or cytochrome *c* detection in untreated cells. Results are representative of three separate experiments.

Figure 8. sHA 14-1 induced cell death is largely caspase independent. RS4;11 cells were incubated with: DMSO, 50 μM Z-VAD-fmk alone, 100 μM isHA 14-1, 1 μM TG, 100 μM sHA 14-1, 100 μM sHA 14-1 + 50 μM Z-VAD, 100 nM ABT-737, or 100 nM ABT-737 + 50 μM Z-VAD. After 18 h cells were stained with PI and Annexin V. The data are shown as the light scatter characteristics on the left side of each condition tested and the PI/ANV staining as contour plots on the right side of each condition tested. PI/ANV analysis was conducted on the cells outlined by the solid line in the light scatter dot plots. The events within the dashed circles in the sHA 14-1 and ABT-737 treated cells are shown to distinguish the difference in light scatter characteristics between the two treated populations.

Figure 1A

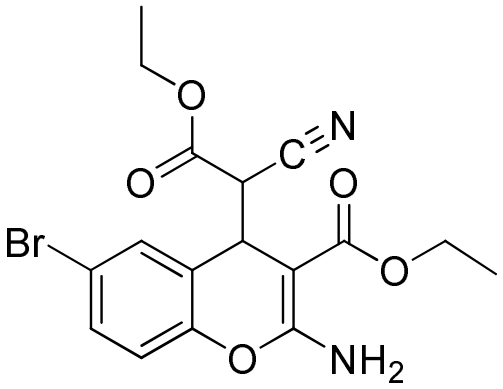

HA 14-1

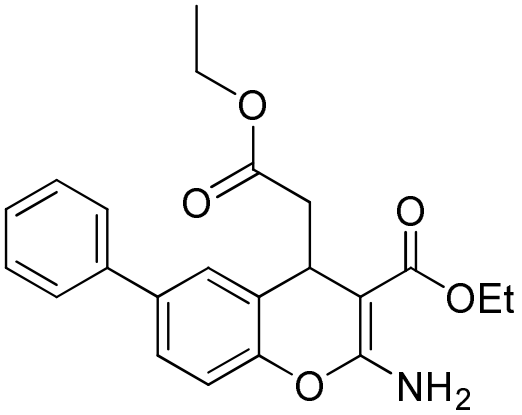

sHA 14-1

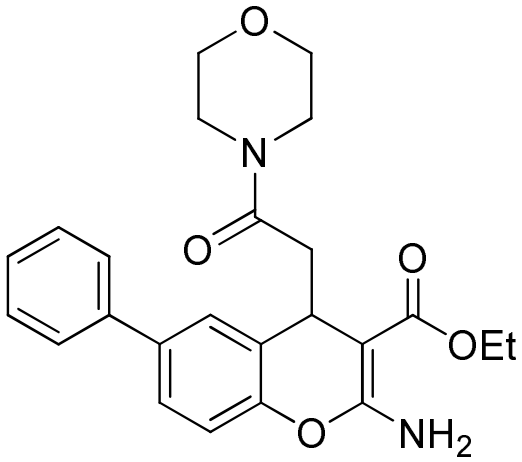

isHA 14-1

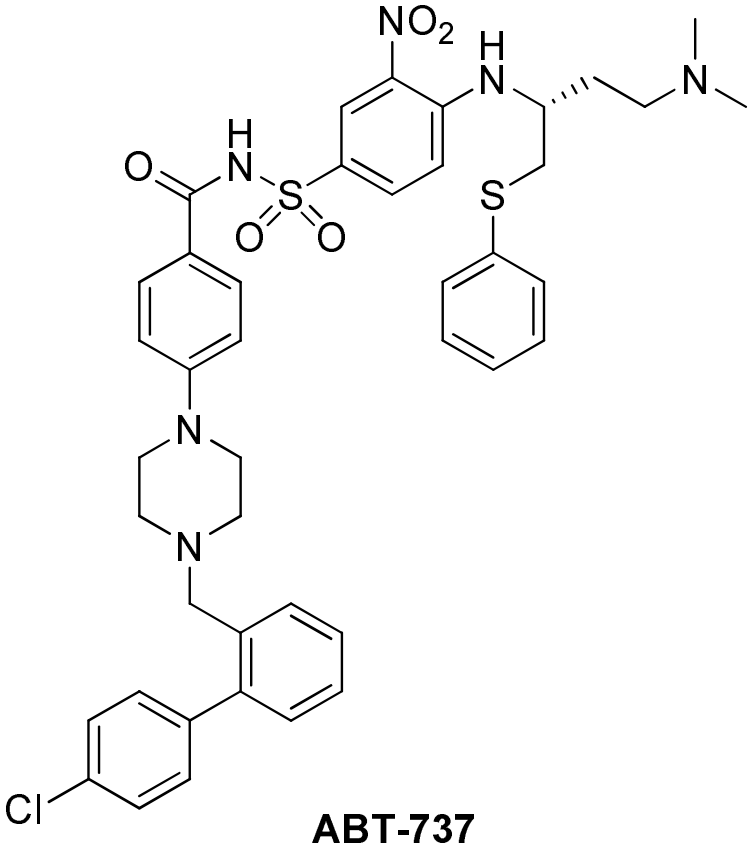

ABT-737

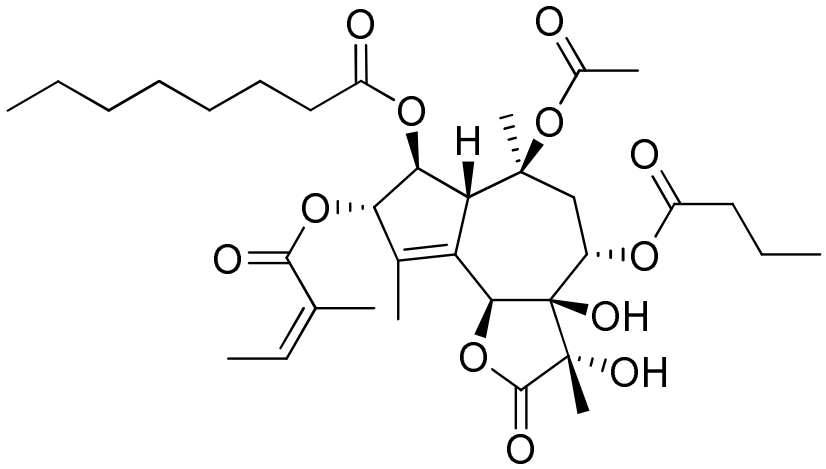

thapsigargin

Molecular Pharmacology Fast Forward. Published on June 26, 2009 as DOI: 10.1124/mol.109.055830
This article has not been copyedited and formatted. The final version may differ from this version.

Figure 1B

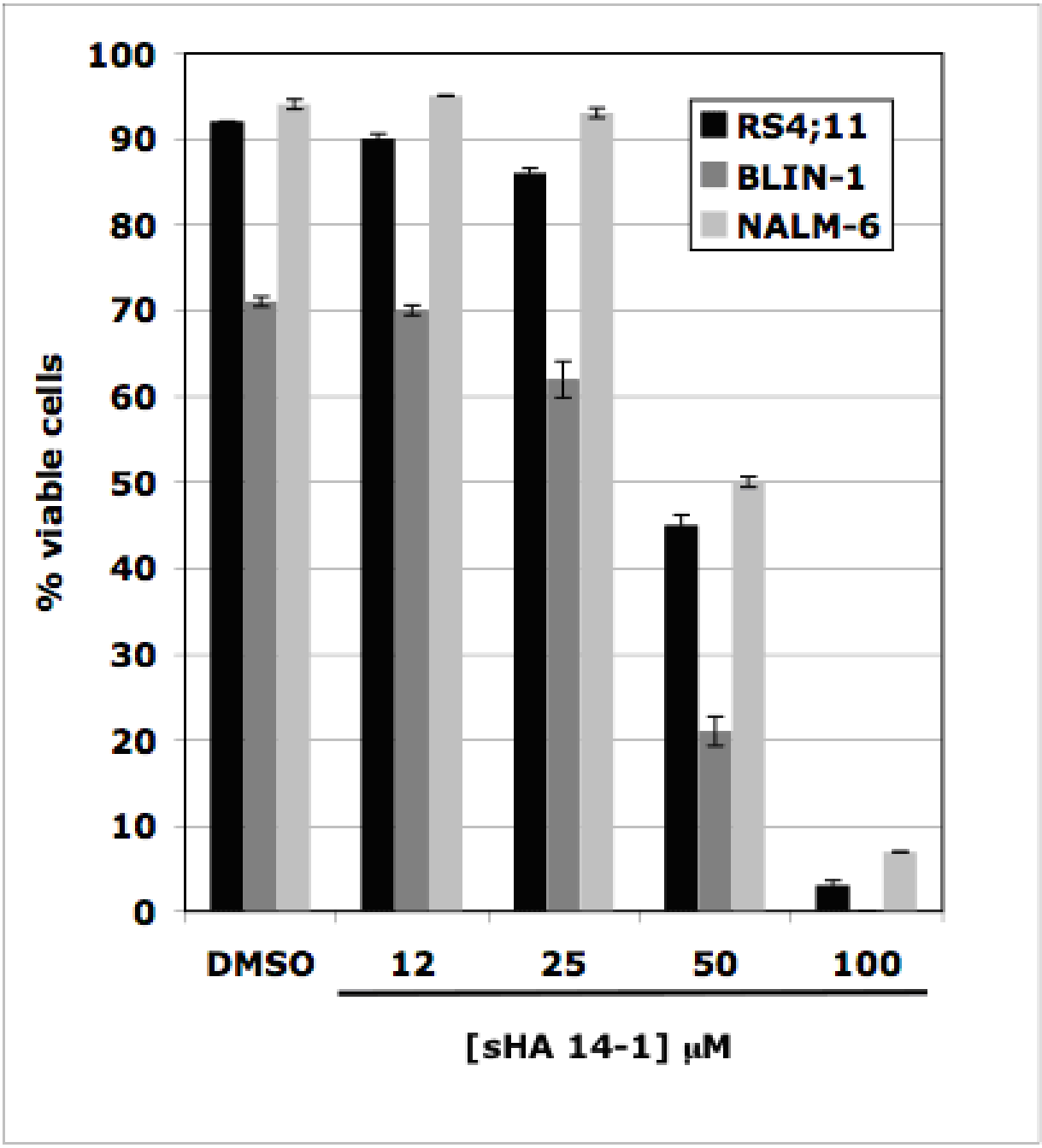

Molecular Pharmacology Fast Forward. Published on June 26, 2009 as DOI: 10.1124/mol.109.055830
This article has not been copyedited and formatted. The final version may differ from this version.

Figure 2A

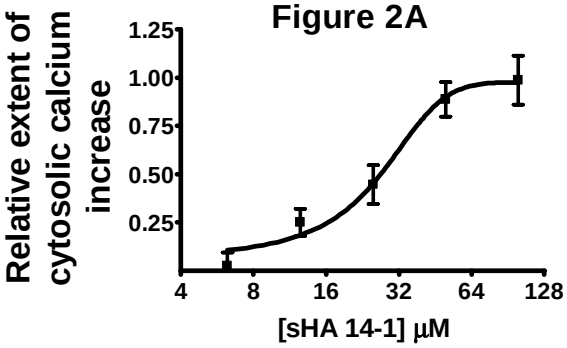

Figure 2B

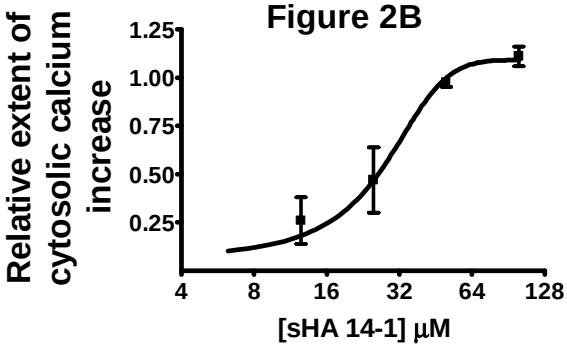

Figure 2C

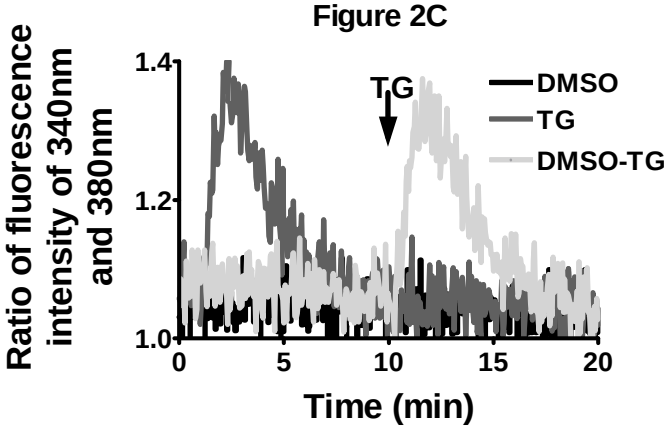

Figure 2D

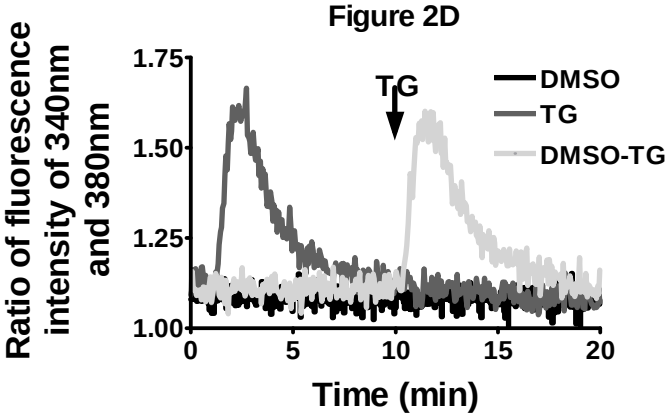

Figure 2E

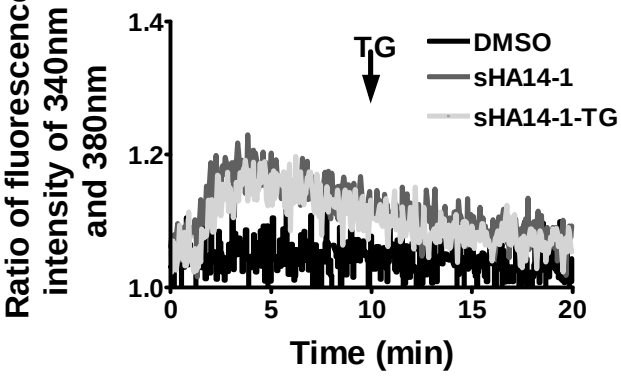

Figure 2F

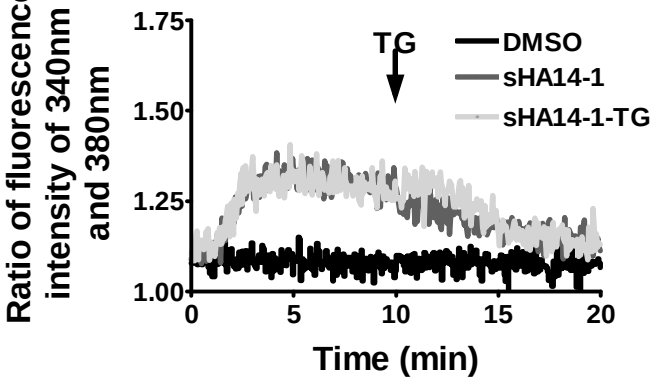

Figure 2G

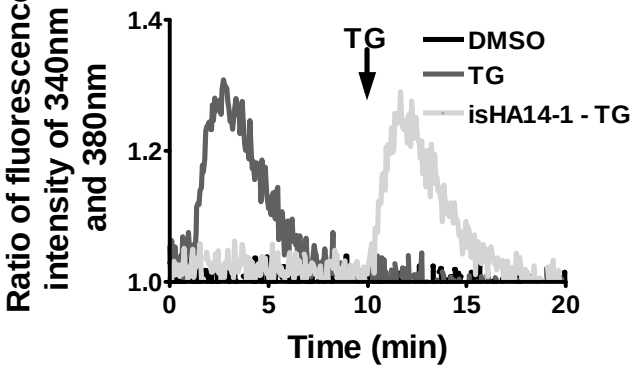

Figure 2H

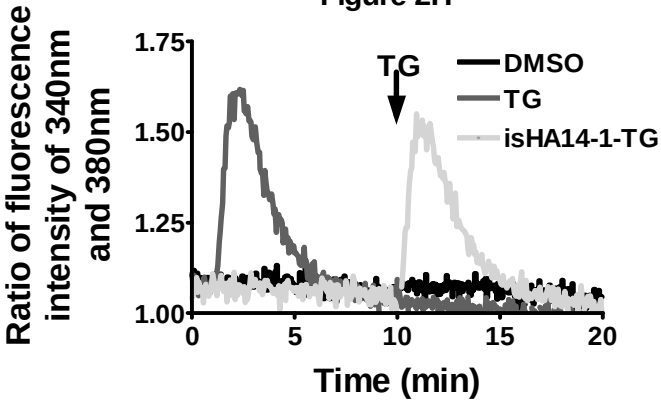

Figure 3

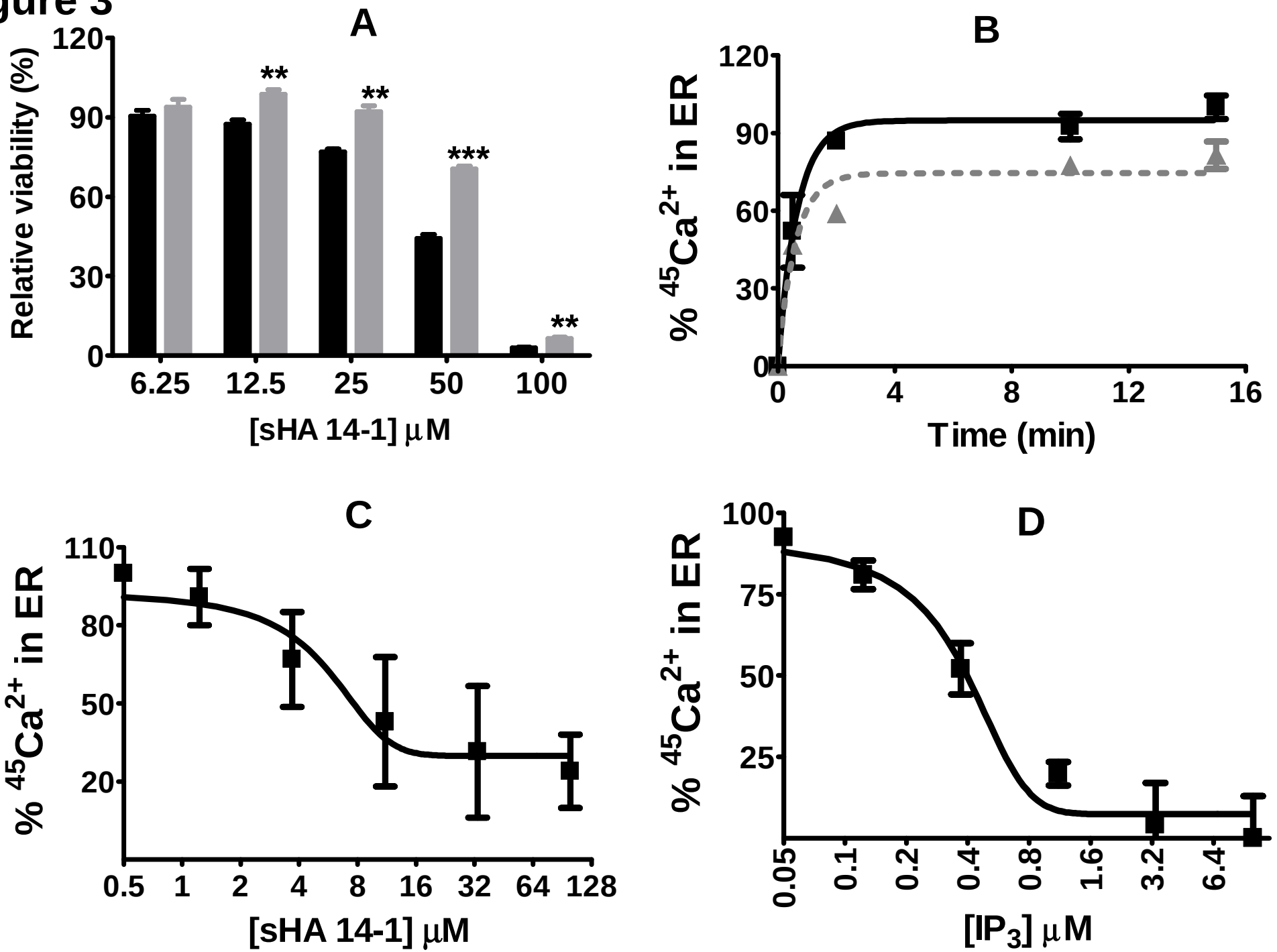

Figure 4

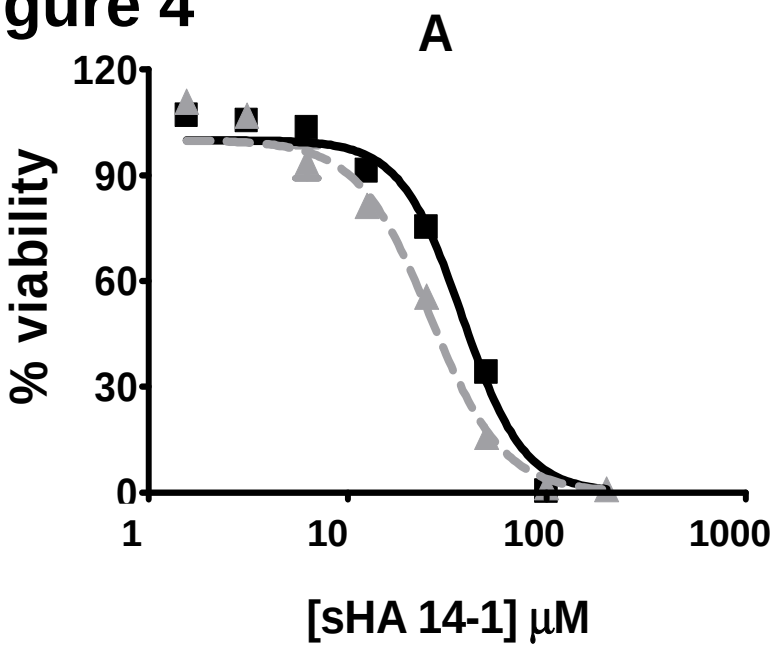

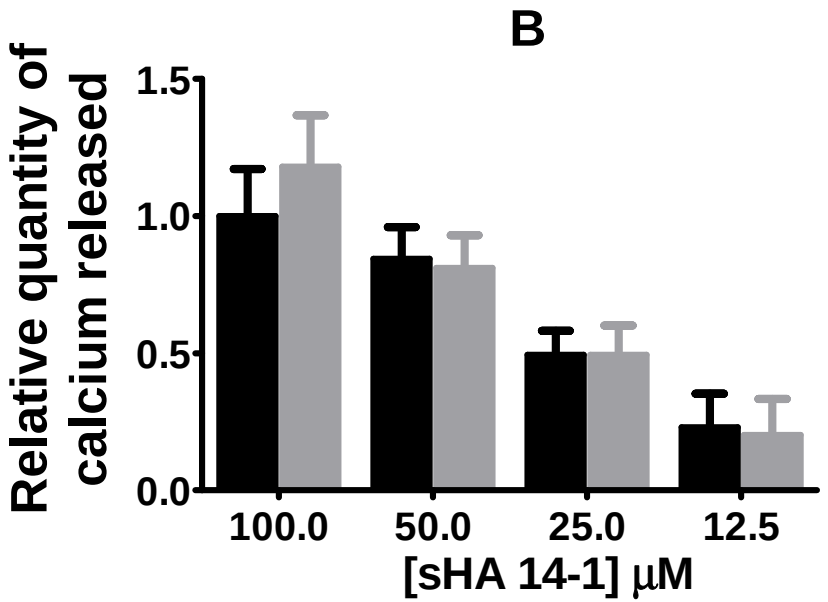

Figure 5

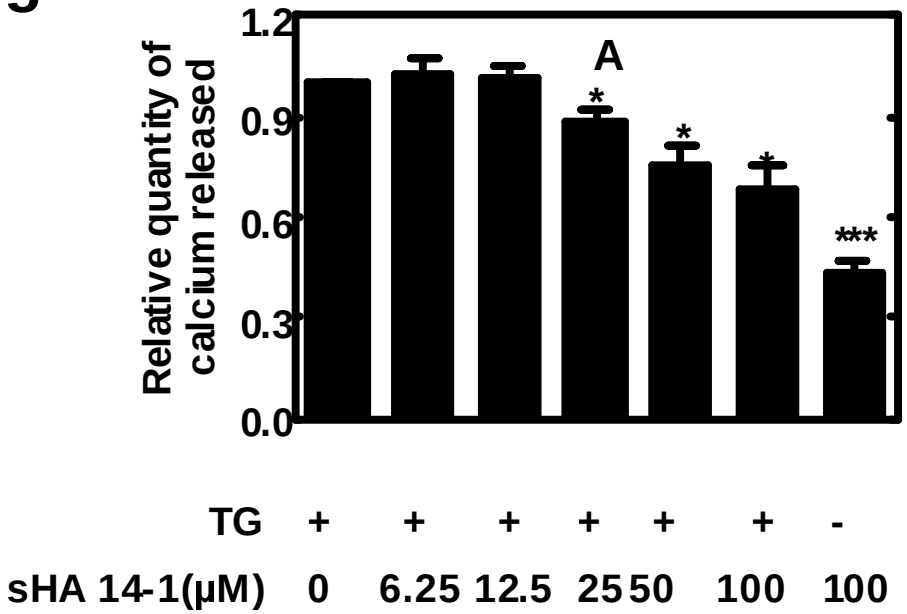

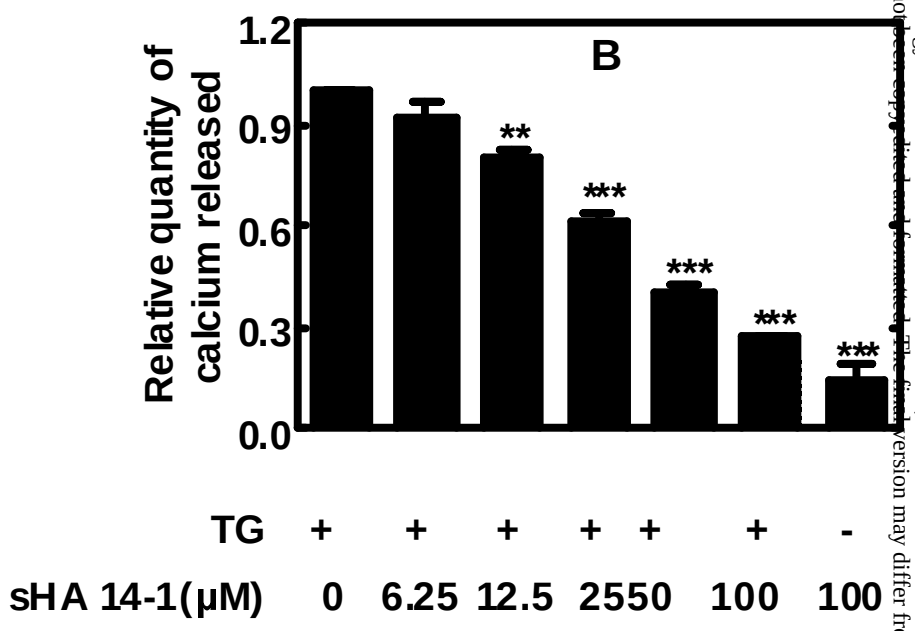

Figure 5

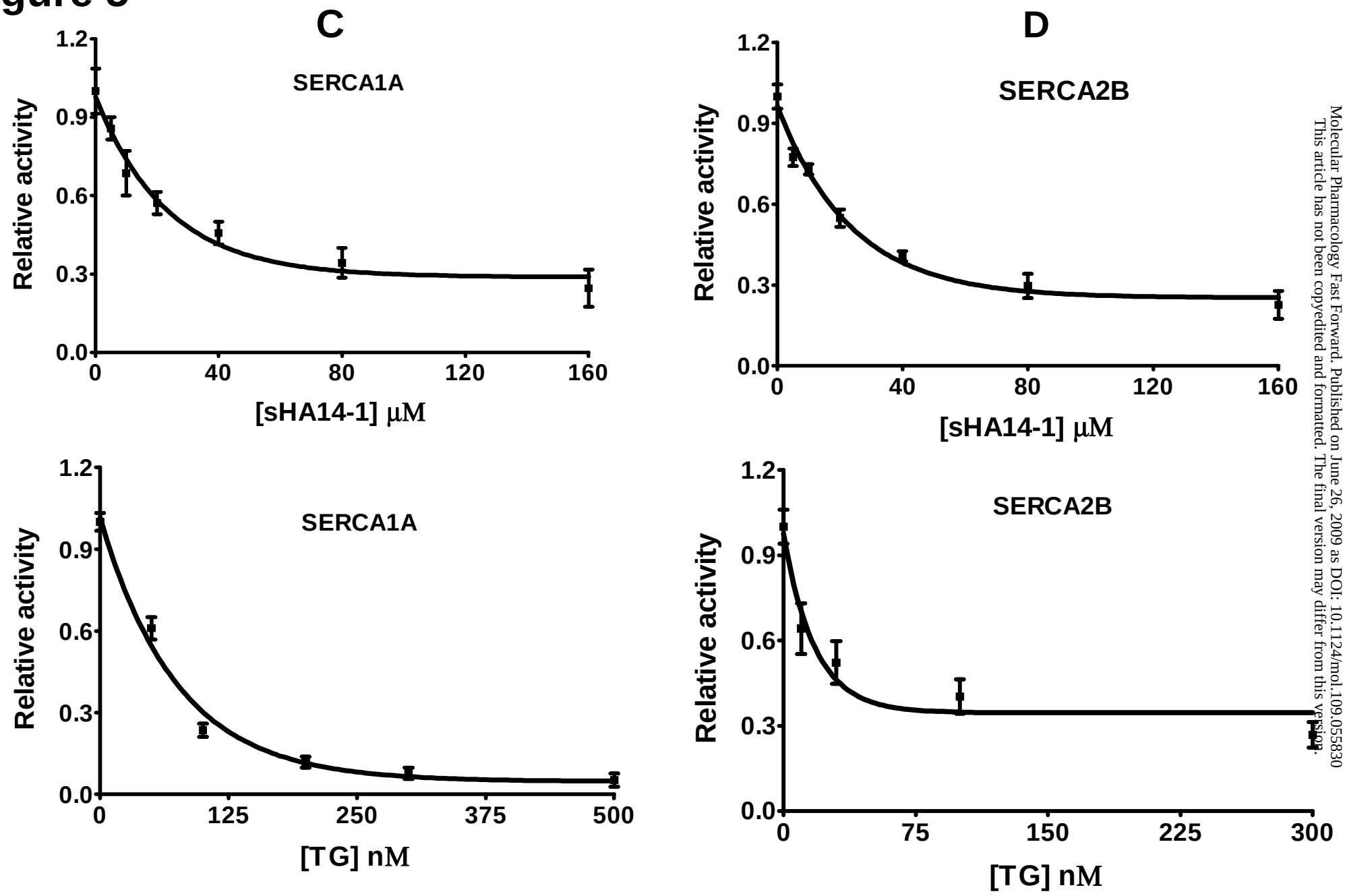

Figure 5

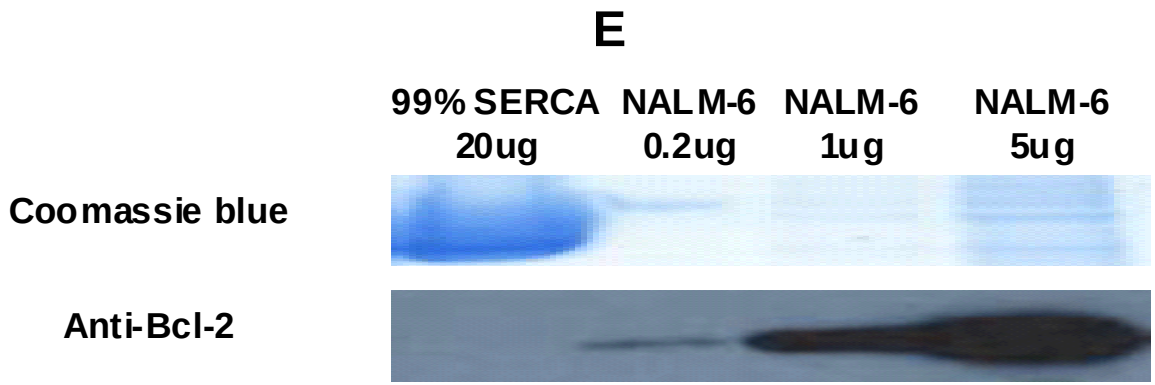

Figure 6

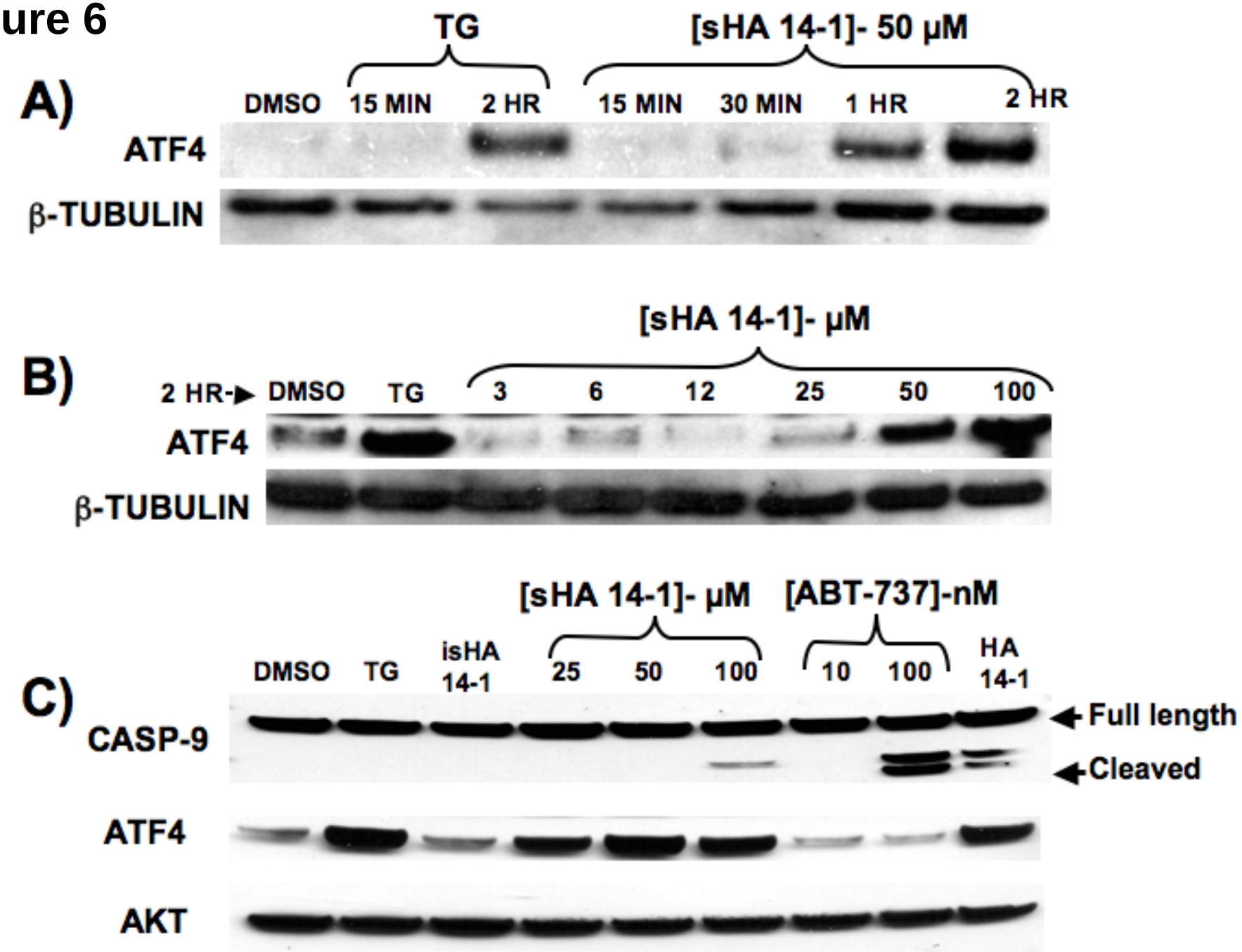

Figure 7

A) NALM-6 (8 h)

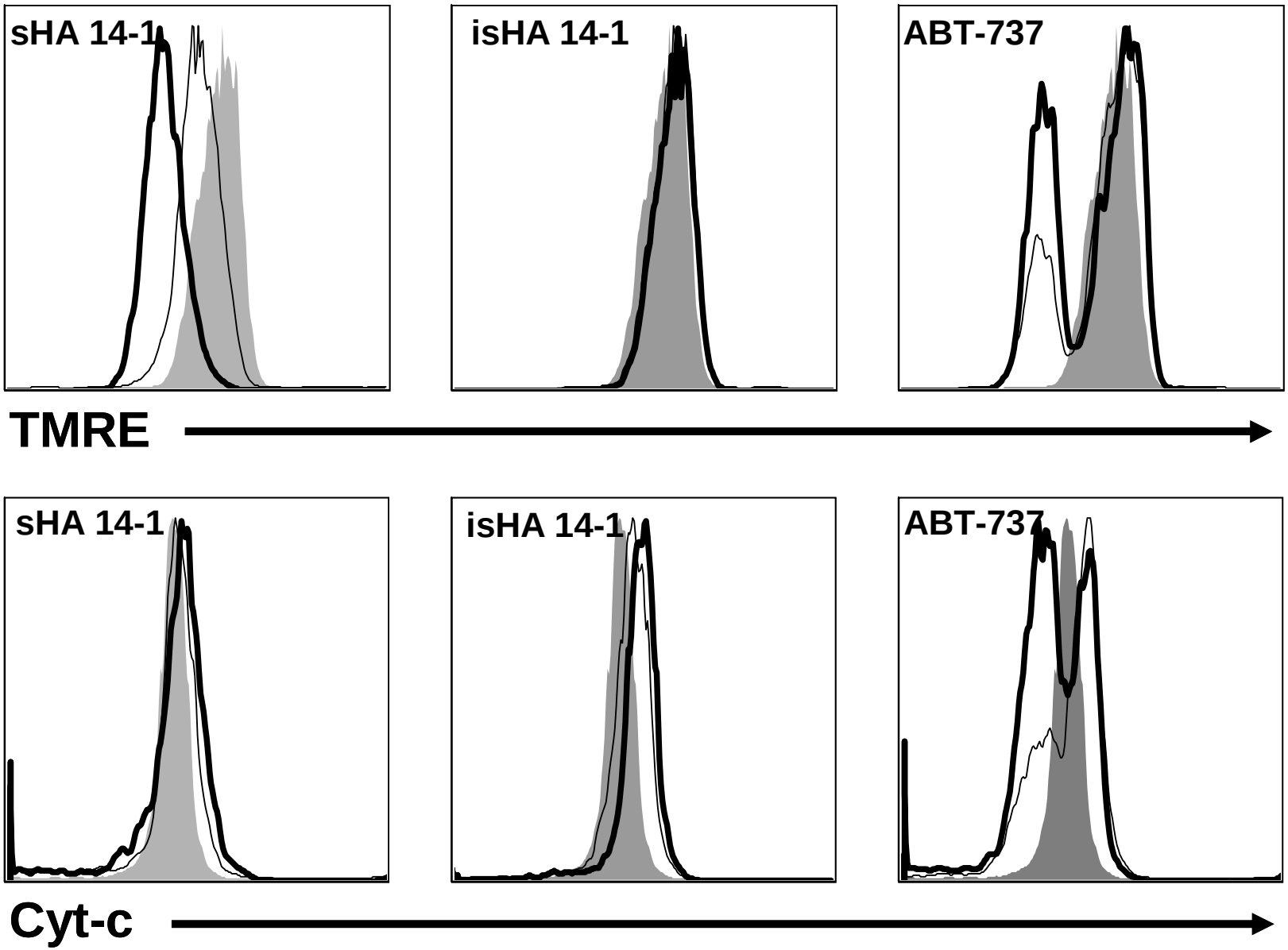

Molecular Pharmacology Fast Forward. Published on June 26, 2009 as DOI: 10.1124/mol.109.055830
This article has not been copyedited and formatted. The final version may differ from this version.

Figure 7

B) RS4;11

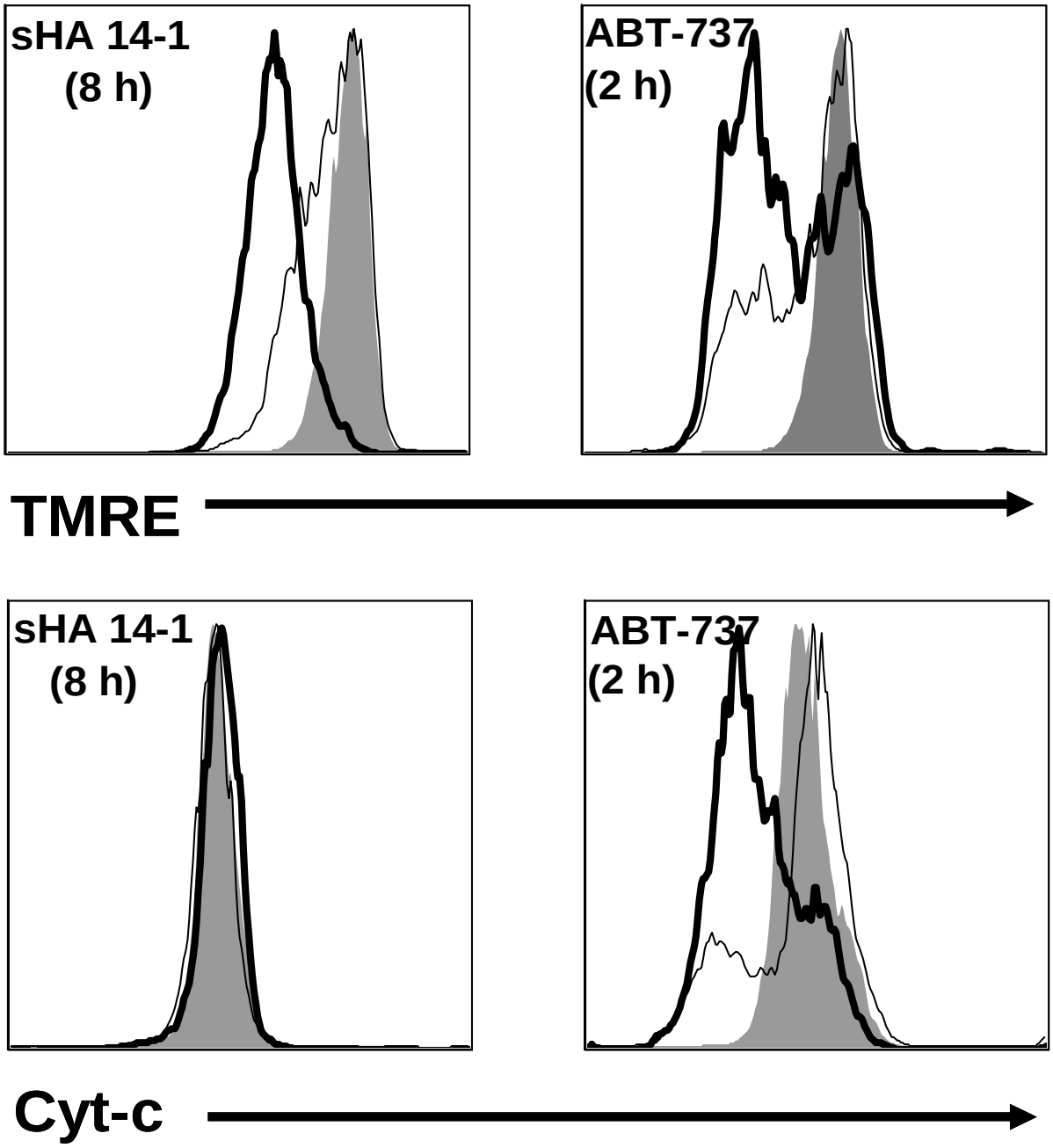

Molecular Pharmacology Fast Forward. Published on June 26, 2009 as DOI: 10.1124/mol.109.055830
This article has not been copyedited and formatted. The final version may differ from this version.

Figure 7

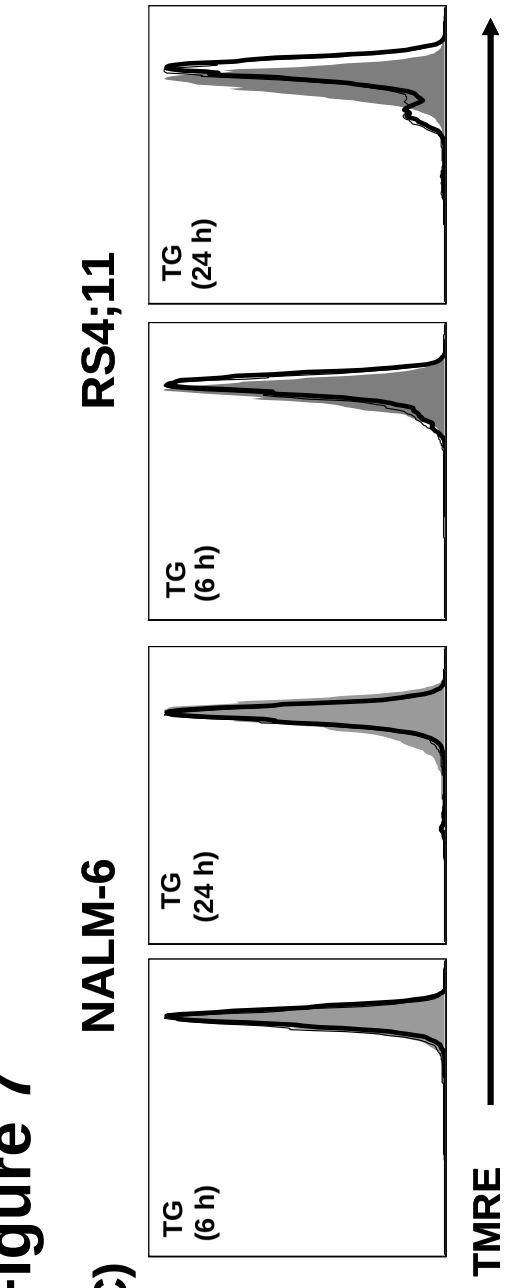

Figure 8

Molecular Pharmacology Fast Forward. Published on June 26, 2009 as DOI: 10.1124/mol.109.055830
This article has not been copyedited and formatted. The final version may differ from this version.